Probing the Saturation Physics via UPC

Amir Rezaeian

UTFSM, Valparaiso

INT Workshop (INT-17-65W), Seattle, February 13 - 17, 2017

Centro Científico Tecnológico de Valparaíso

UNIVERSIDAD TECNICA FEDERICO SANTA MARIA

Outline:

- DIS and exclusive VM production at small-x.
- Signature of gluon saturation/CGC in UPCs at HERA and the LHC.
- Exclusive dijet production in coherent diffractive processes in UPCs.

Unified description of inclusive & exclusive processes in color-dipole factorization

Exclusive diffractive process: $\psi^{\gamma}_{q\bar{q}} \otimes \mathcal{N} \otimes \phi^{V}_{q\bar{q}}$

$t^{q\bar{q}}_{\text{life}} >> t^{q\bar{q}}_{\text{int}}$

contains all small-x physics, multiple scatterings

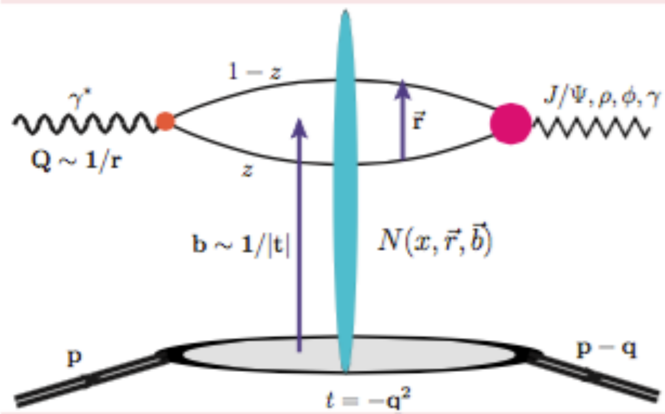

$$\mathcal{A}^{\gamma^* p \to Vp}_{T,L}(x, Q, \Delta) = 2\mathrm{i} \int \mathrm{d}^2\vec{r} \int_0^1 \mathrm{d}z (\Psi^*_E \Psi)_{T,L} \int \mathrm{d}^2\vec{b}\, \mathrm{e}^{-\mathrm{i}[\vec{b}-(1-z)\vec{r}]\cdot\vec{\Delta}} N(x, r, b)$$

$$\frac{\mathrm{d}\sigma^{\gamma^* p \to Ep}_{T,L}}{\mathrm{d}t} = \frac{1}{16\pi} \left| \mathcal{A}^{\gamma^* p \to Ep}_{T,L} \right|^2 \qquad t = -\Delta^2$$

- With corrections from the real part of the amplitude and skewedness effect $x \neq x'$
- $(b \to 1/|t|)$: t-distributions access impact-parameter distribution of interactions

Inclusive deep-inelastic scattering (DIS): $\psi^{\gamma}_{q\bar{q}} \otimes \mathcal{N} \otimes \psi^{\gamma}_{q\bar{q}}$

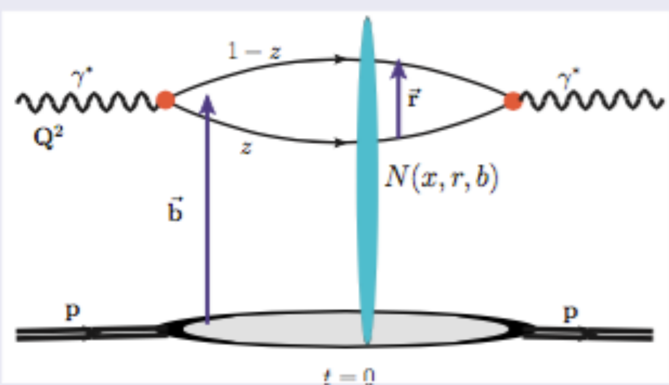

$$\sigma^{\gamma^* p}_{L,T}(Q^2, x) = Im\, \mathcal{A}^{\gamma^* p \to \gamma^* p}_{T,L}(x, Q, \Delta = 0)$$

$$= 2 \int \mathrm{d}^2\vec{r} \int_0^1 dz\, |\Psi_{L,T}(r, z; Q^2)|^2 \int \mathrm{d}^2\vec{b}\, N(x, r, b)$$

- DIS is less sensitive to the b-dependence compared to exclusive diffractive process

and **does not** probe $b \approx 0$, but $b \approx 2 \div 3\, \mathrm{GeV}^{-1}$.

Unified description of inclusive & exclusive processes in color-dipole factorization

Exclusive diffractive process: $\psi^{\gamma}_{q\bar{q}} \otimes \mathcal{N} \otimes \phi^{V}_{q\bar{q}}$

contains all small-x physics, multiple scatterings

$$t^{q\bar{q}}_{\rm life} >> t^{q\bar{q}}_{\rm int}$$

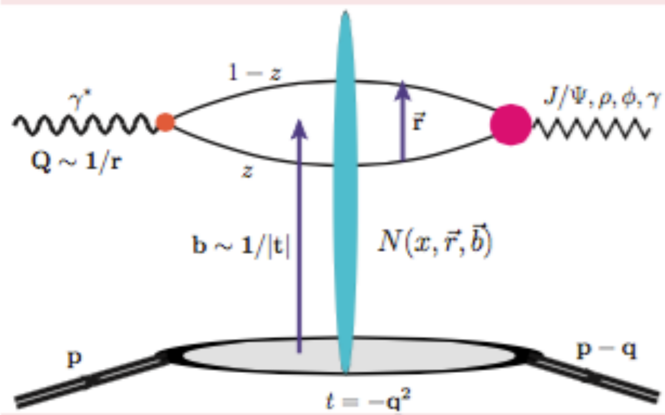

$$\mathcal{A}^{\gamma^* p\to Vp}_{T,L}(x,Q,\Delta) = 2i\int d^2\vec{r}\int_0^1 dz(\Psi^*_E\Psi)_{T,L}\int d^2\vec{b}\, e^{-i[\vec{b}-(1-z)\vec{r}]\cdot\vec{\Delta}} N(x,r,b)$$

$$\frac{d\sigma^{\gamma^* p\to Ep}_{T,L}}{dt} = \frac{1}{16\pi}\left|\mathcal{A}^{\gamma^* p\to Ep}_{T,L}\right|^2 \qquad t=-\Delta^2$$

- With corrections from the real part of the amplitude and skewedness effect $x \neq x'$
- $(b \to 1/|t|)$: t-distributions access impact-parameter distribution of interactions

Inclusive deep-inelastic

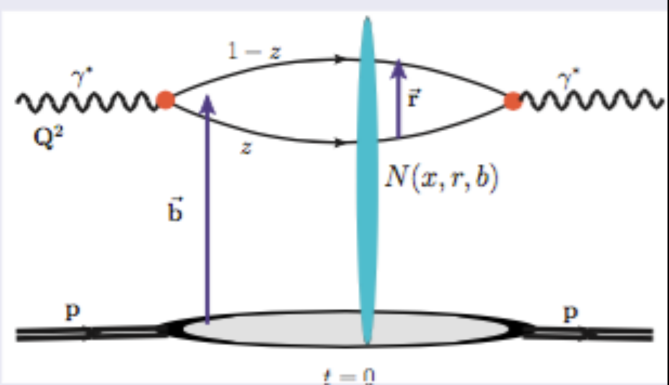

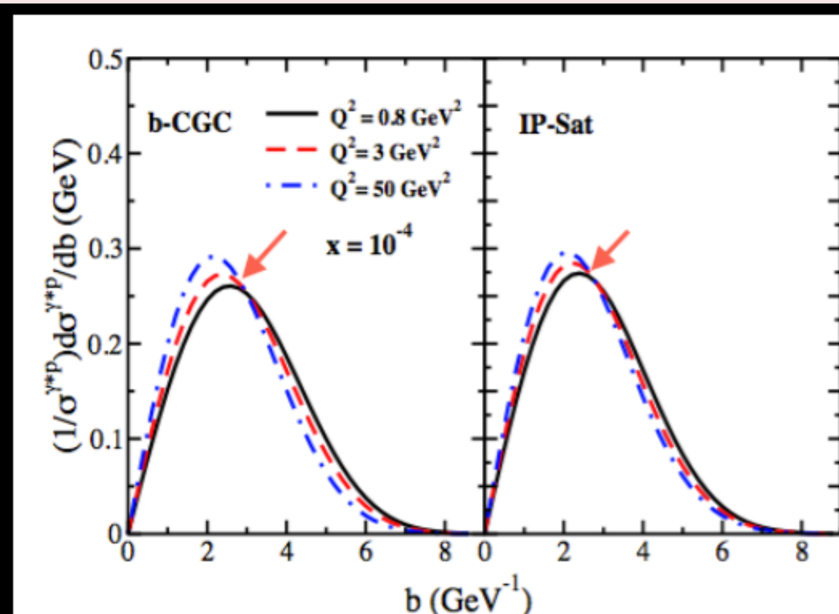

b-dependence of saturation scale and t-distribution of diffractive processes

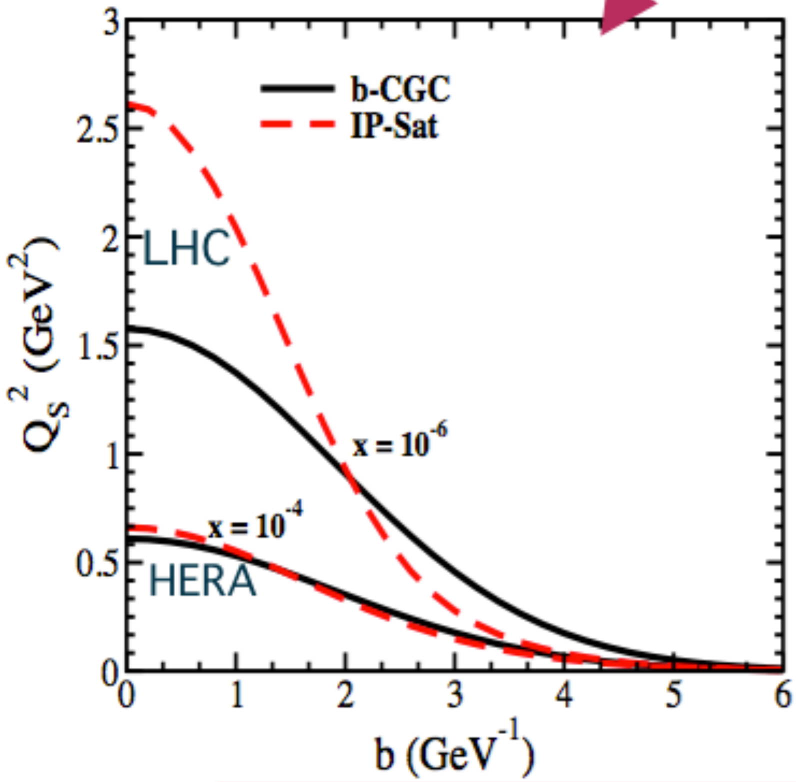

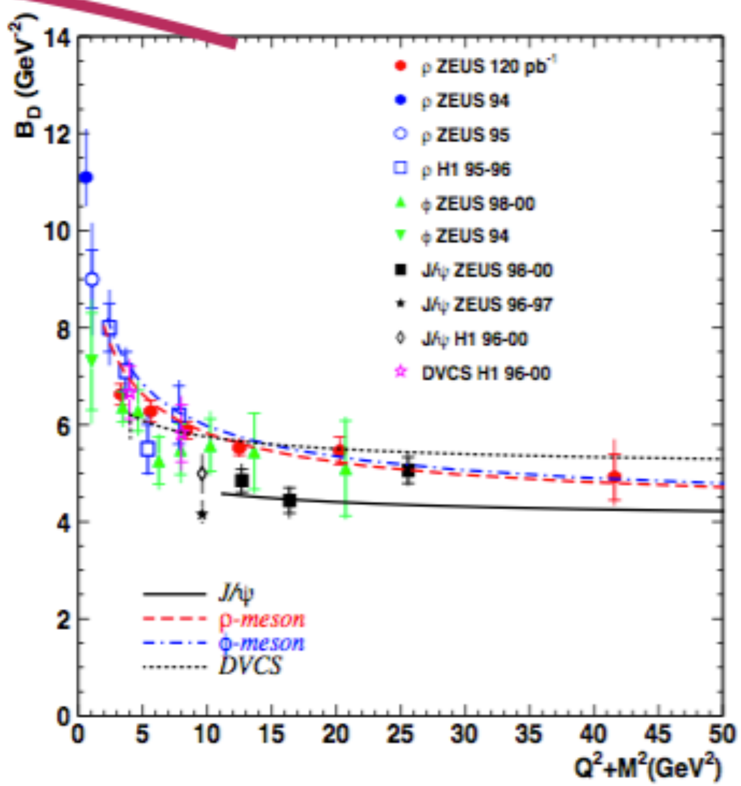

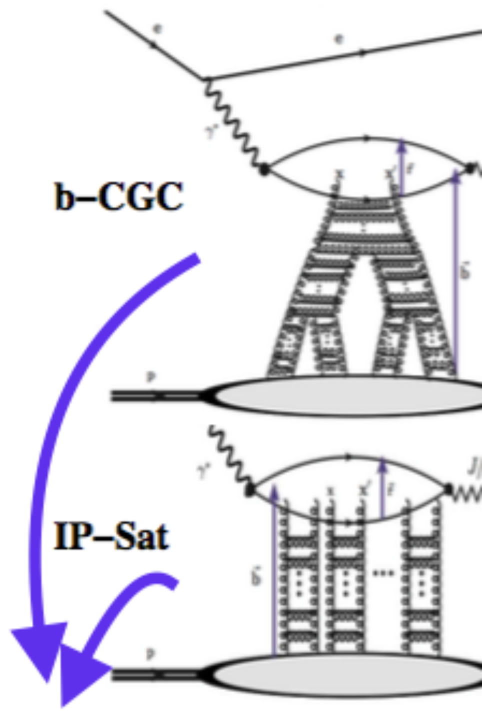

$$\frac{d\sigma_{T,L}^{\gamma^* p \to Ep}}{dt} \approx e^{-B_D|t|} \; (\text{large } Q^2) \Longleftrightarrow Q_s^2(x,b) \approx Q_s^2(x) e^{-b^2/2B_D}$$

- At a fixed Q^2, the typical dipole size is bigger for lighter vector meson $\Longrightarrow$ validity of the above asymptotic expression is postponed to a higher Q^2.
- t-**slope** B_D **gives the width of saturation scale distribution in proton.**

A unified description of combined inclusive HERA data & diffractive data in CGC

Rezaeian, Siddikov, Van de Klundert, Venugopalan, arXiv:1212.2974; Rezaeian, Schmidt, arXiv:1307.0825

The dipole scattering amplitude is the main ingredient with 3 or 4 free parameters fixed via a fit to the reduced cross–section.

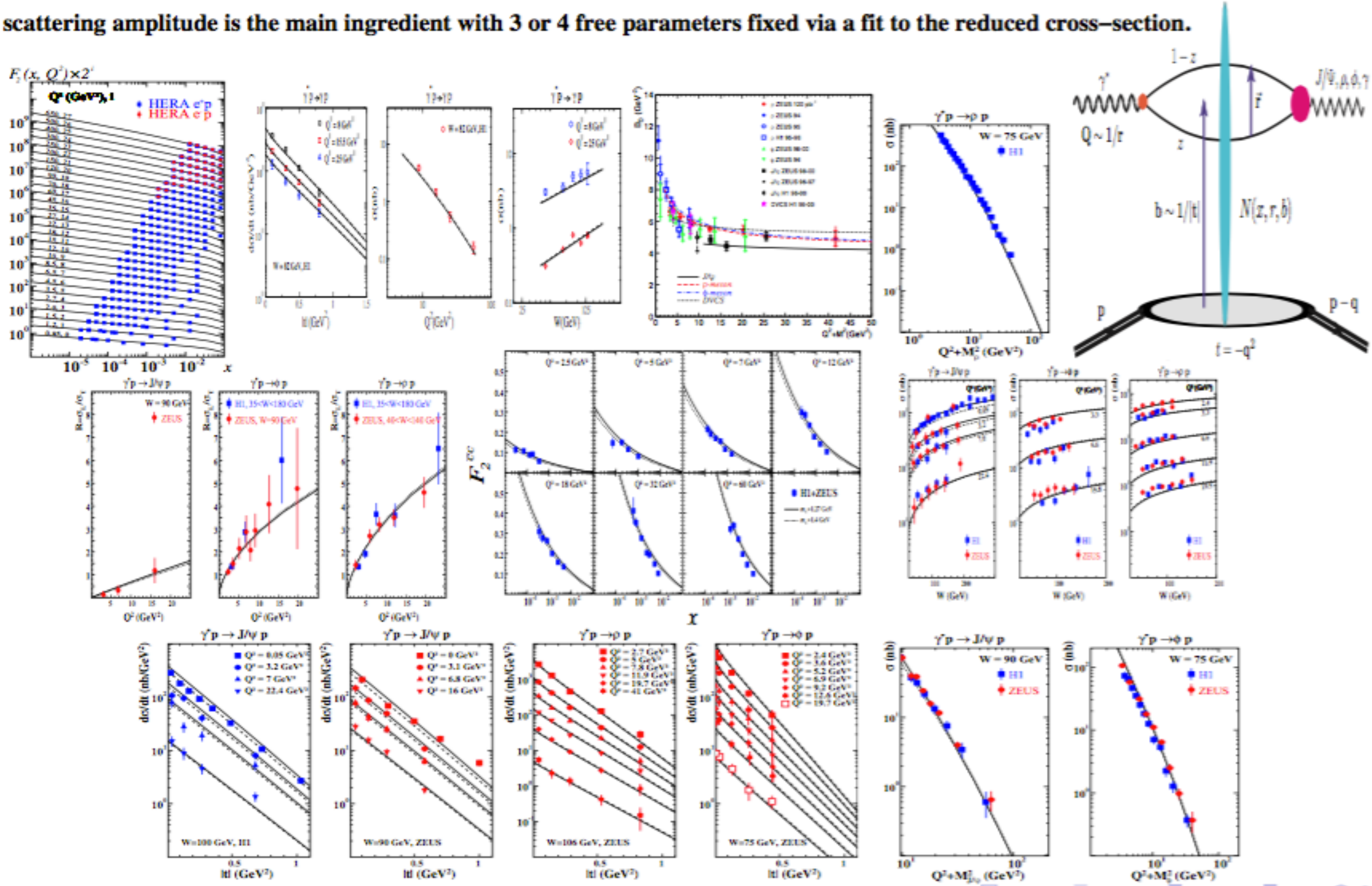

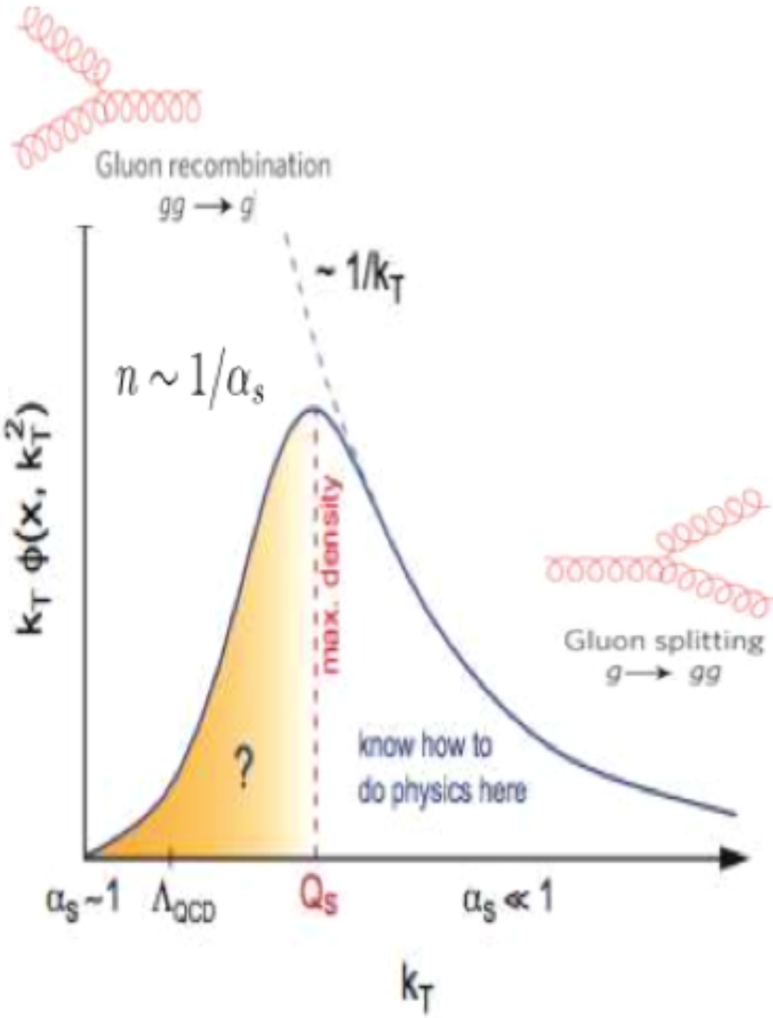

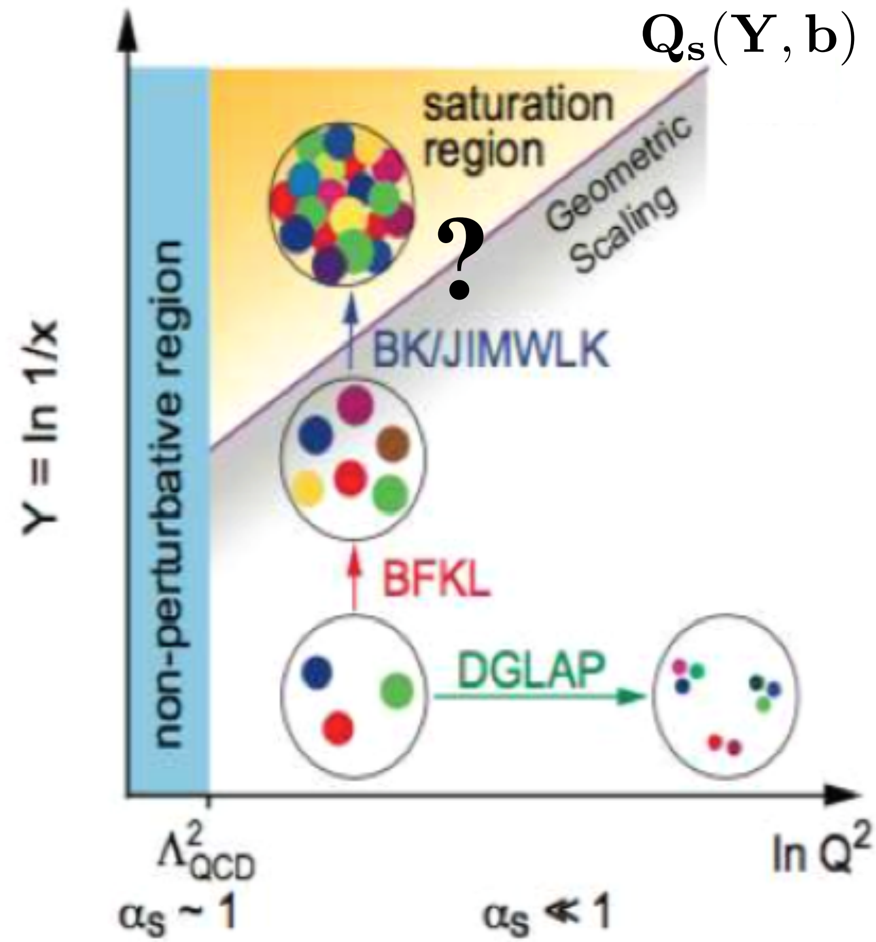

- Is the CGC perturbative approach reliable & systematic at the small-x?

  Is the saturation scale large enough?

The impact-parameter *b* and *x*- dependence of the saturation scale for proton

Rezaeian and Schmidt, arXiv:1307.0825

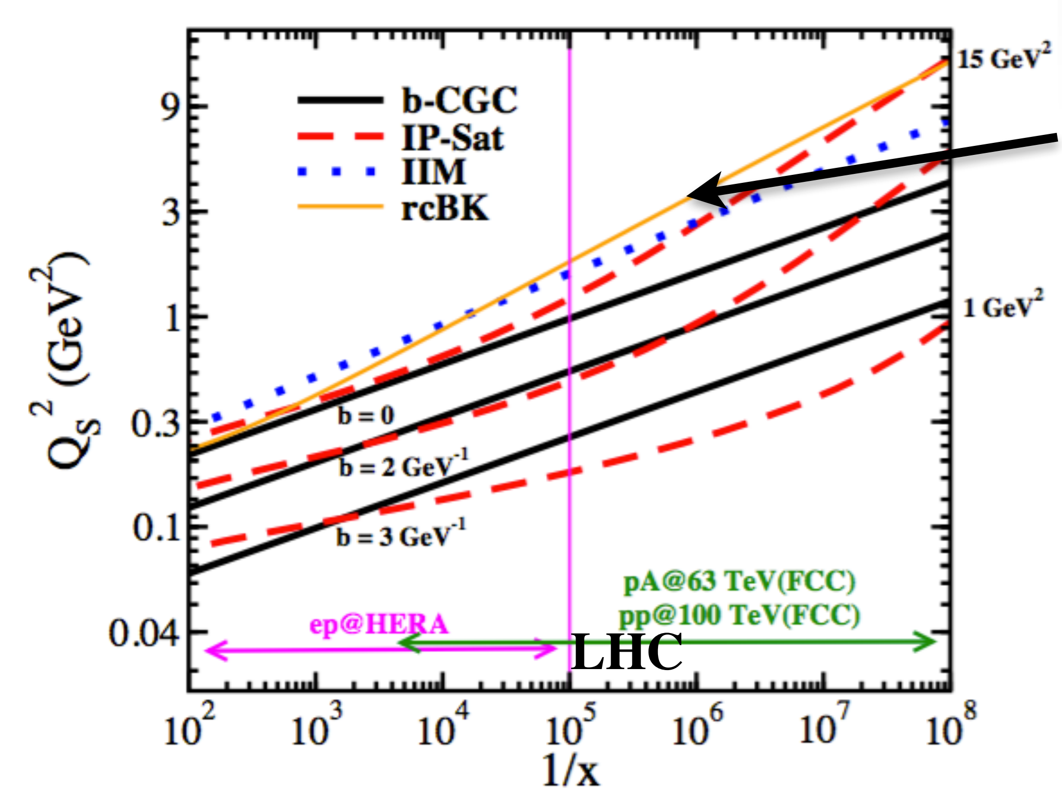

- **b-independent saturation models significantly overestimate Q_s.**

- **Proton saturation scale:**

$$\mathrm{HERA} : Q_s < 1\,\mathrm{GeV}$$

$$\mathrm{LHC} : Q_s \leq 1 - 2\,\mathrm{GeV}$$

$$\mathrm{FCC} : Q_s \leq 2 - 4\,\mathrm{GeV}$$

- **Nuclear saturation scale:** $Q_{sA}^2 \approx A^{1/3} Q_s^2 \approx 6\, Q_s^2$

$$\mathrm{EIC} : Q_{sA} < 2.5\,\mathrm{GeV}$$

CGC (IP-Sat v. b-CGC) description of combined HERA data

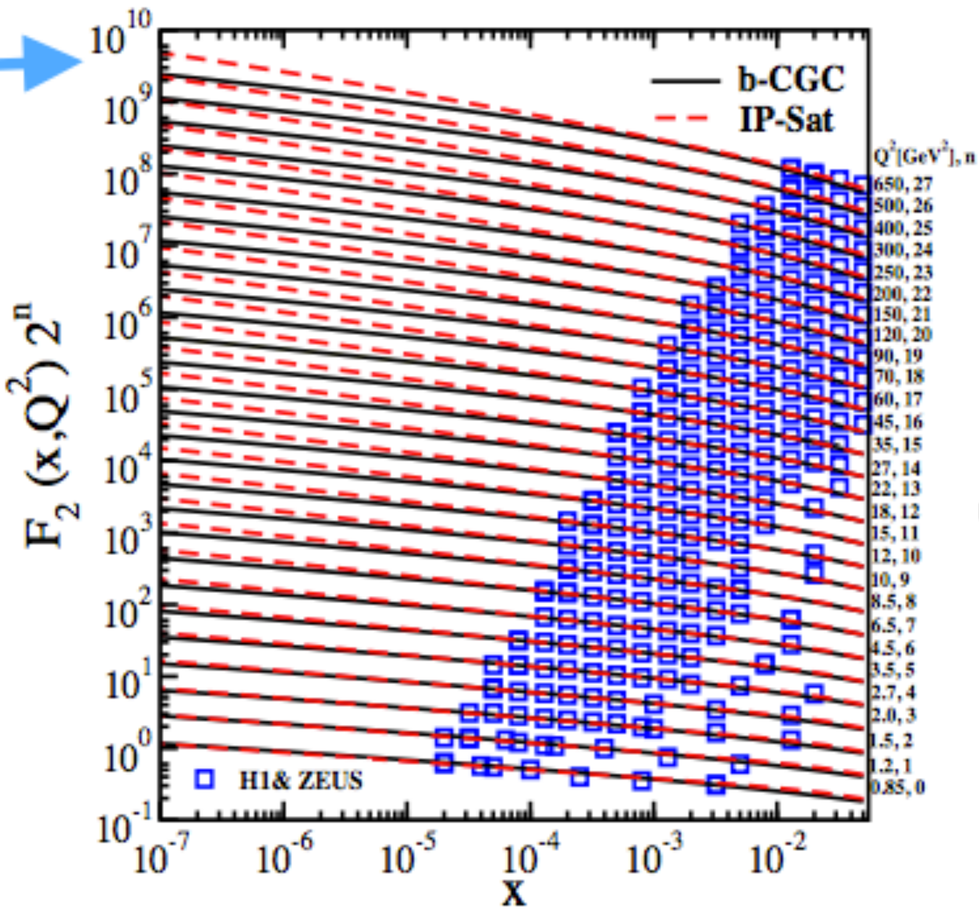

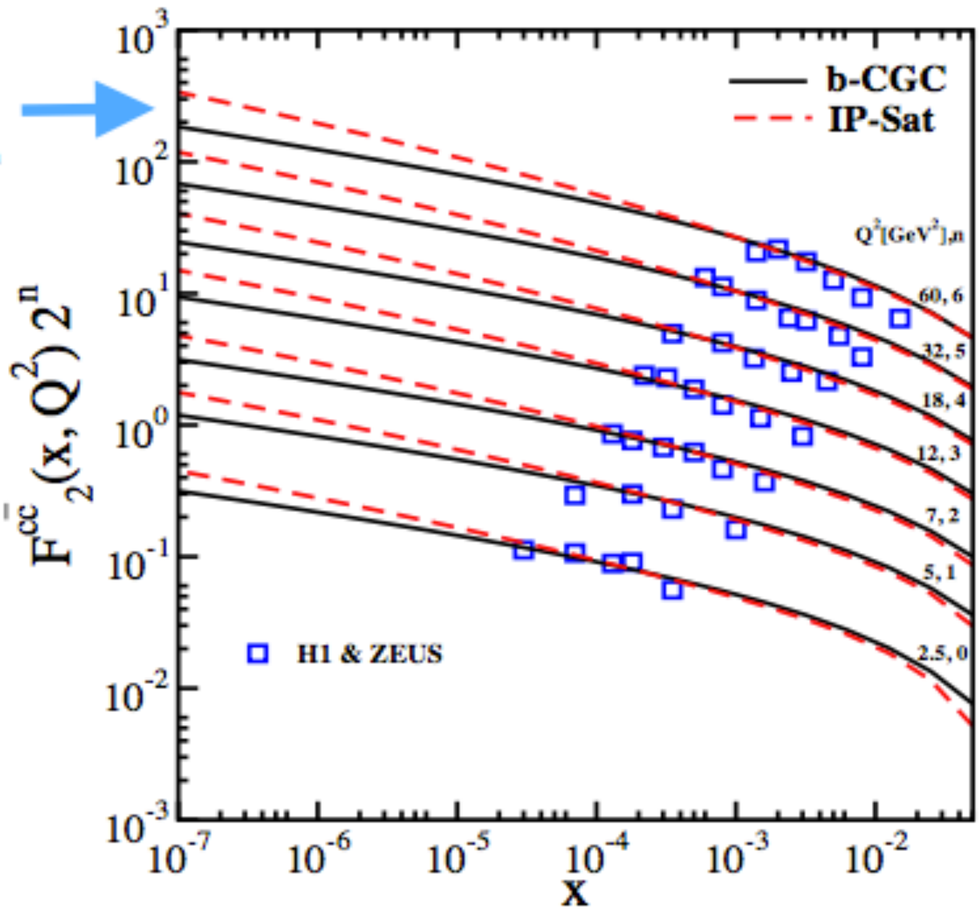

FCC ← **LHC**

Cross-validation

- $F_{c\bar{c}}$, F_2 data were not included in the fit. → *No biased, No over-fitted.*
- The difference among models can be considered as our current theoretical uncertainties $\Longrightarrow$ significant uncertainties at small-x $\Longrightarrow$ Future exps with $x_B < 10^{-5}$ (LHeC, FCC) can constrain saturation models.

Photo-vector-meson production in ultra-peripheral collisions at LHC

▸ **U**ltra-**P**eripheral **C**ollision: limit $Q^2 = 0$

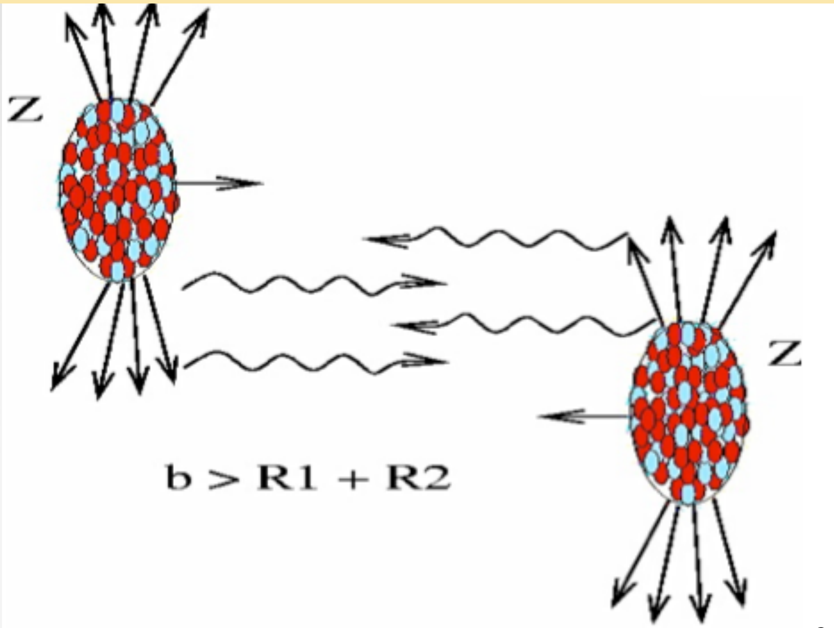

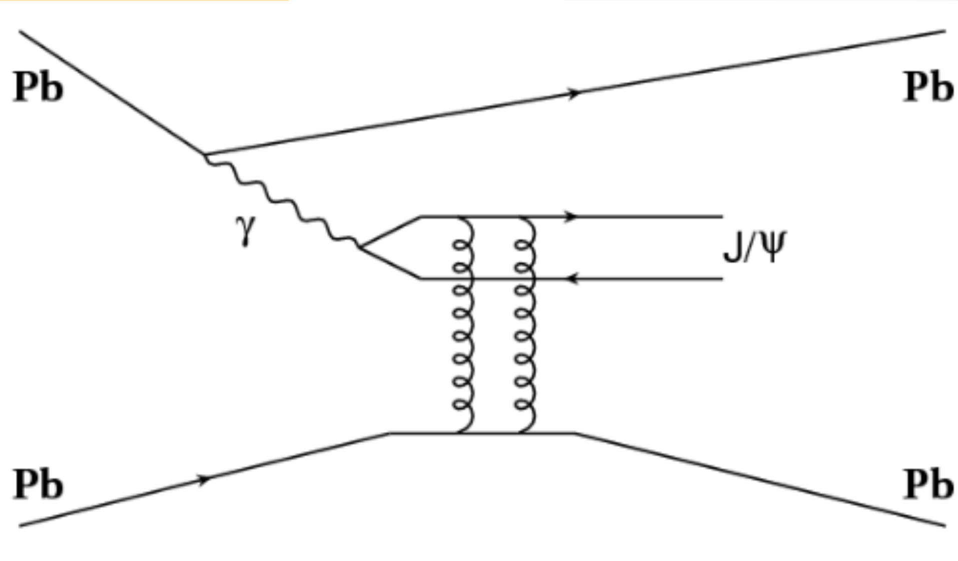

$W_{\gamma p} = 3\,\text{TeV in pp@LHC} \rightarrow x_B \approx 10^{-6}$

UPC's give a strong constraint on gluons at small x (10^{-3}-10^{-5}), but . . .

❑ pQCD:

- **Factorization theorem (is not universal) for exclusive cross section ~ $xg(x,Q^2)^2$.**
- **No full NLO calculation, scheme dependent (scale,…)**
- **Cannot currently be used in a global PDF analysis.**

❑ CGC:

- **Factorization is universal for different vector mesons.**
- **No full NLO calculation.**
- **Can be used to constrain small-x physics.**

Photonuclear vector meson production in ultra-peripheral collisions at LHC

Without nuclear effects

Color dipole models (modeling nuclear Q_s?)

With nuclear gluon shadowing

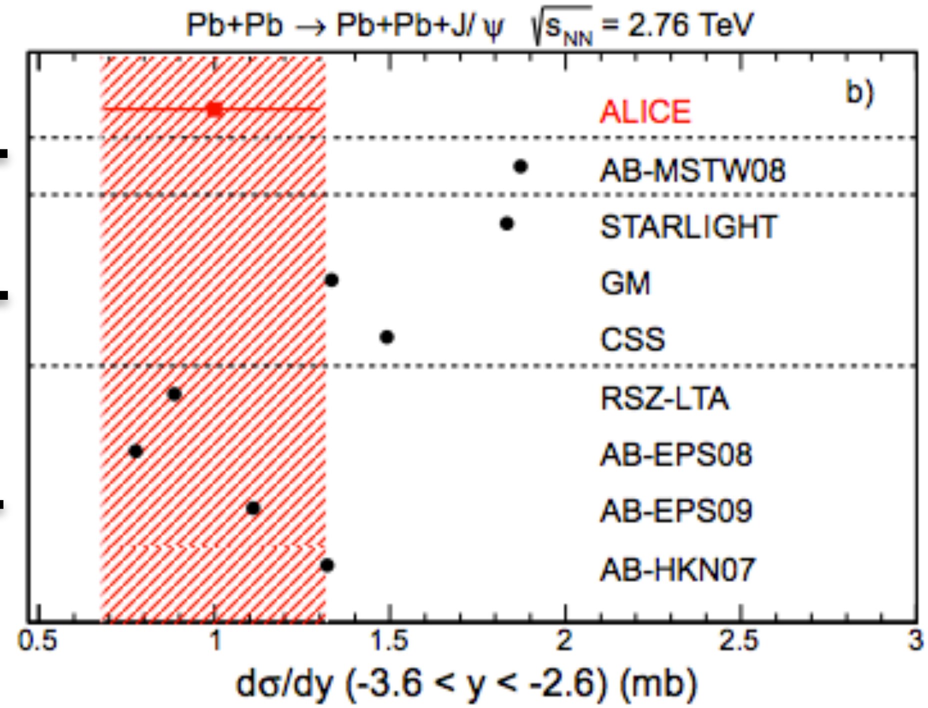

Rebyakova, Strikman and Zhalov (RSZ): the nuclear gluon distribution in the leading twist approximation, PLB 710 (2012) 647.

➢ **ALICE conclusión (arXiv:1209.3715):**

The cross section cannot be understood from a simple scaling of the nucleon cross section neglecting nuclear effects. Best agreement is seen with models which include nuclear gluon shadowing.

Photonuclear vector meson production in ultra-peripheral collisions at LHC

Without nuclear effects

Color dipole models
(modeling nuclear Q_s?)

With nuclear gluon shadowing

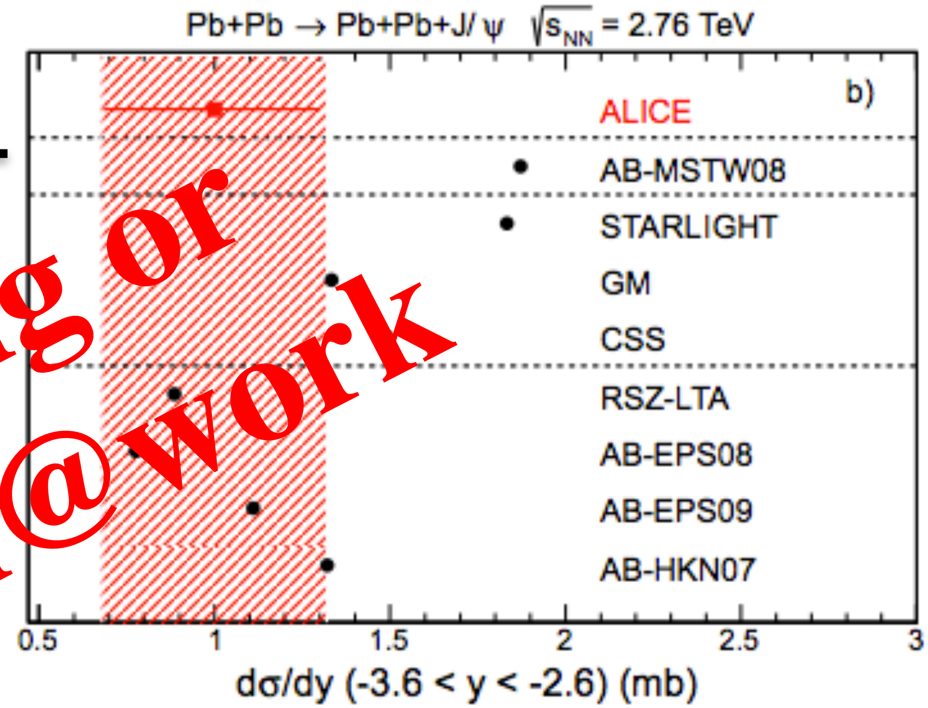

Shadowing or saturation@work

Rebyakova, Strikman and Zhalov (RSZ): the nuclear gluon distribution in the leading twist approximation, PLB 710 (2012) 647.

➢ ALICE conclusión (arXiv:1209.3715):

The cross section cannot be understood from a simple scaling of the nucleon cross section neglecting nuclear effects. Best agreement is seen with models which include nuclear gluon shadowing.

Photo-production of J/ψ from HERA to the LHC

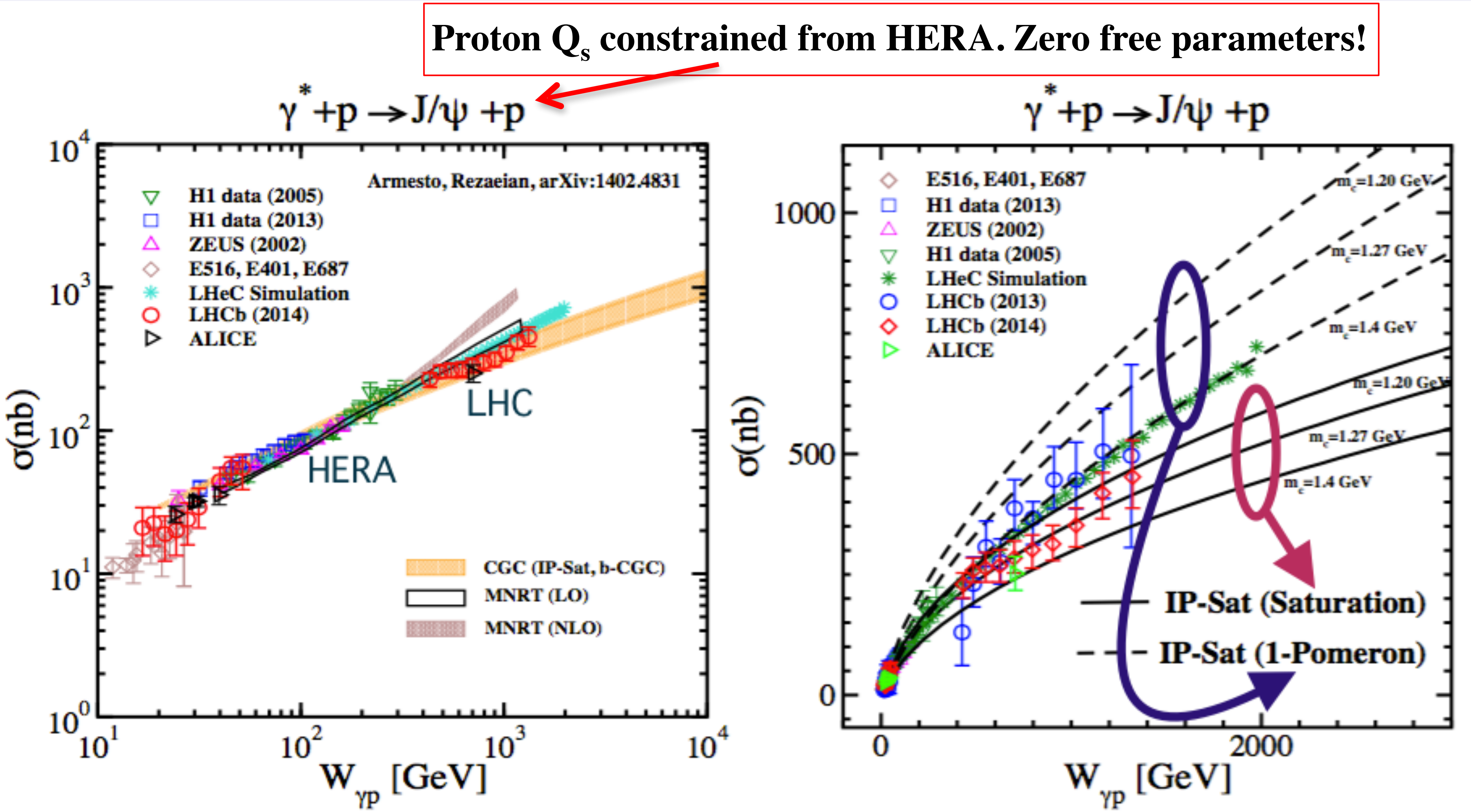

- The LHCb and ALICE data seem to favor the CGC/Saturation predictions.
- The uncertainties related to the charm mass is very large.

Photonuclear Ψ(2S) production in ultra-peripheral collisions at LHC

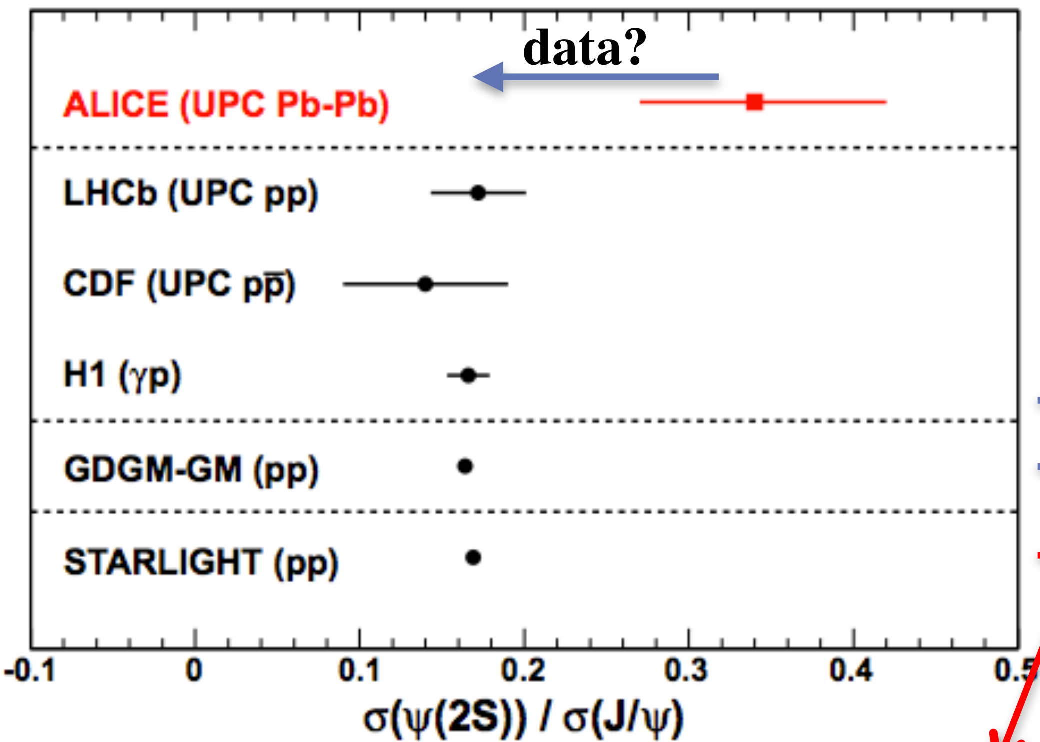

arXiv:1508.05076

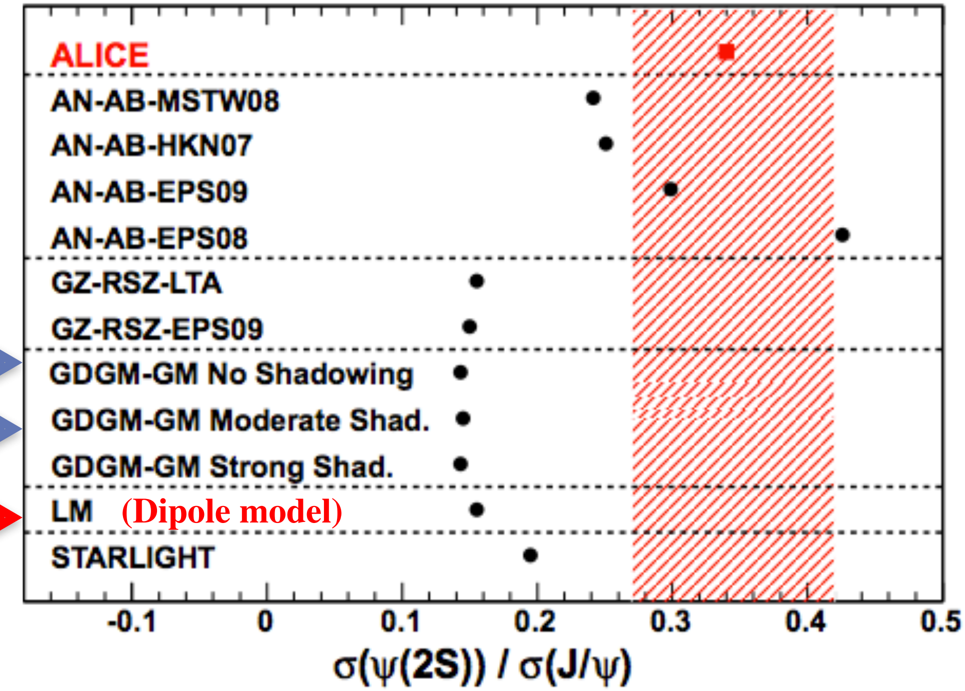

Lappi and Mäntysaari, arXiv:1301.4095

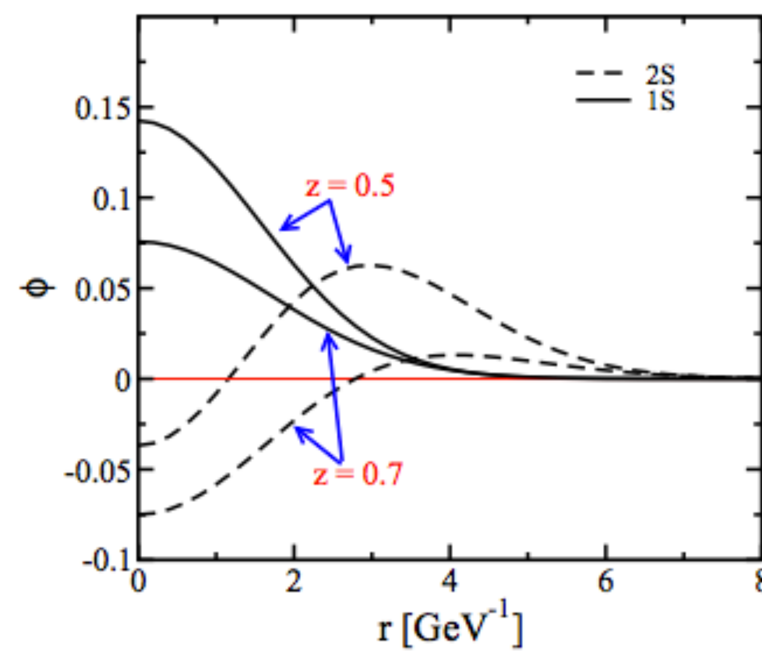

- ✦ Ψ(2S) wave function has a node and is heaver than J/Ψ
  → Large suppression compared to J/Ψ.
- ✦ The Ψ(2S) wave function is less known.

Data remain to be understood?

Photonuclear Ψ(2S) production in ultra-peripheral collisions at LHC

ALICE, arXiv:1508.05076

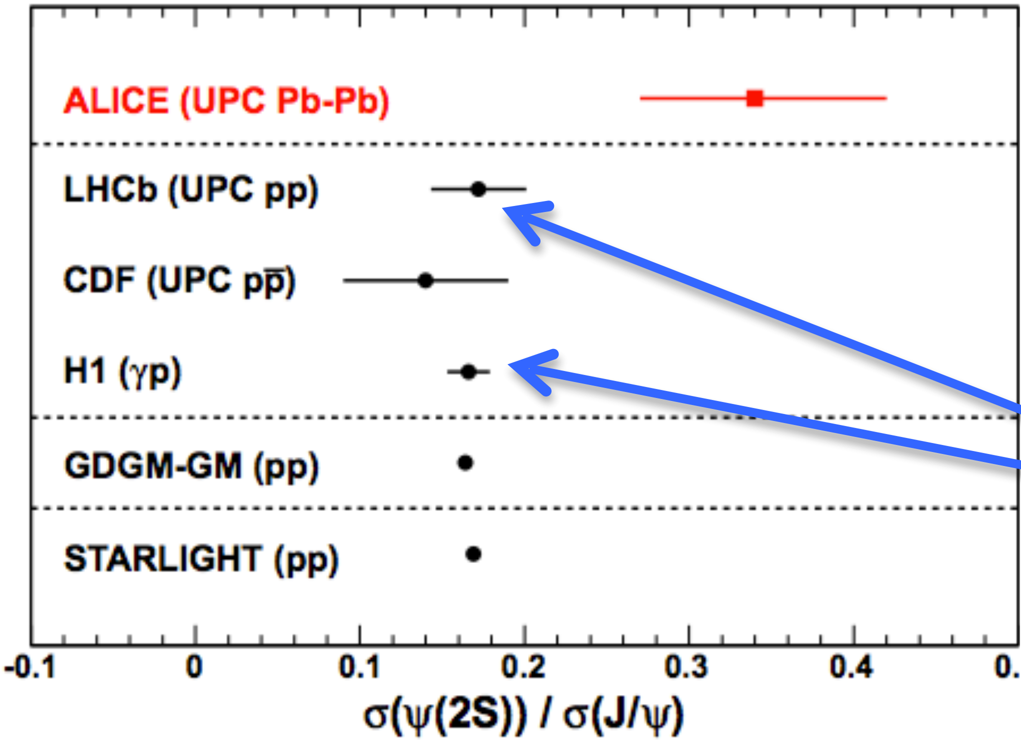

Armesto, AR, arXiv:1402.4831

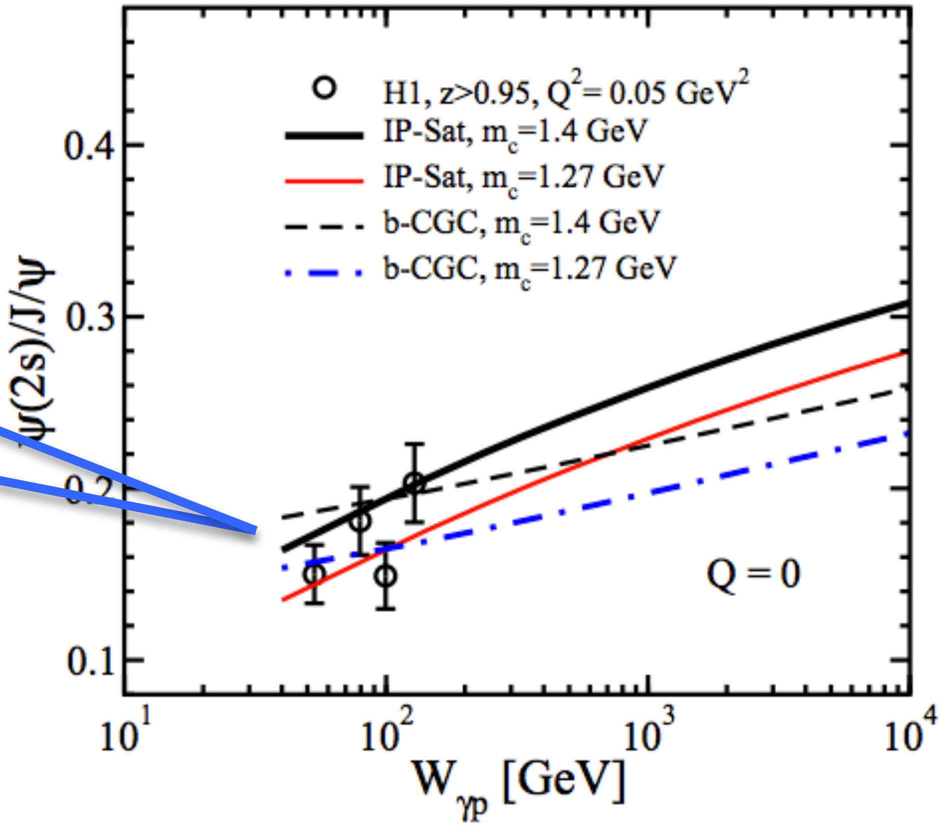

- ➢The ratio is certainly energy-dependent!.
- ➢The energy-dependence of the ratio can be a good test of the color-dipole picture!.

Diffractive dijet v. inclusive dijet in UPC

Diffractive (averaging over color at amplitude level): $\sigma \propto |\langle \mathcal{M} \rangle_\rho|^2$
Inclusive (averaging over color at cross-section level): $\sigma \propto \langle |\mathcal{M}|^2 \rangle_\rho$

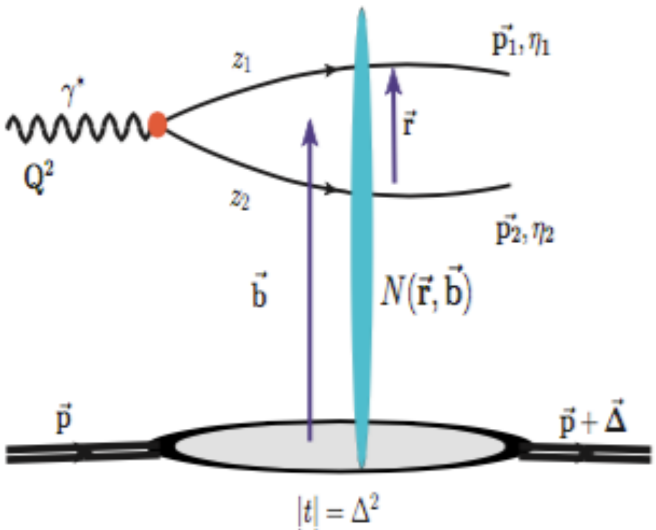

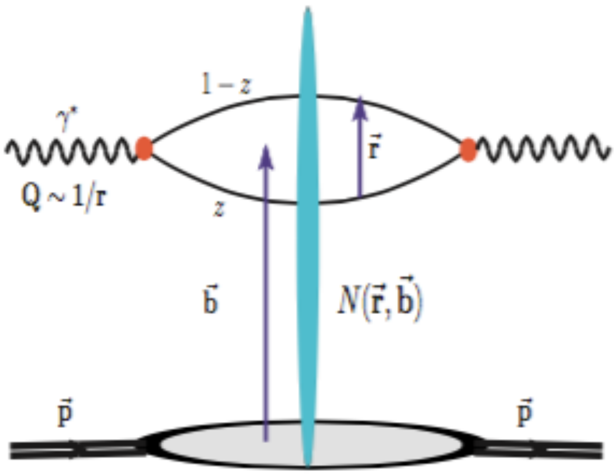

Dominguez, Marquet, Xiao, Yuan, arXiv:1101.0715

Altinoluk, Armesto, Beuf, Rezaeian, arXiv:1511.07452

$$\sigma^{\text{Diffractive dijet}} \propto \psi^{\gamma}_{q\bar{q}} \otimes \mathcal{N}(\vec{r}, \vec{b}) \otimes \mathcal{N}(\vec{r'}, \vec{b'}) \neq \psi^{\gamma}_{q\bar{q}} \otimes [\mathcal{N}(r, b)]^2$$

$$\sigma^{\text{Inclusive dijet}} \propto \psi^{\gamma}_{q\bar{q}} \otimes [\mathcal{N}(\vec{r}, \vec{b}) + S^{\text{Quadrupole}}(\vec{r}, \vec{r\prime}, \vec{b}, \vec{b'})]$$

$$\sigma^{\text{Inclusive DIS}} \propto \psi^{\gamma}_{q\bar{q}} \otimes \mathcal{N}(\vec{r}, \vec{b})$$

- In contrast to inclusive dijet production, diffractive dijet production only depends on the dipole amplitude (not WW gluon distribution) at LO.

Diffractive Dijet production in the CGC: $\gamma^* + p(A) \to q\bar{q} + p(A)$

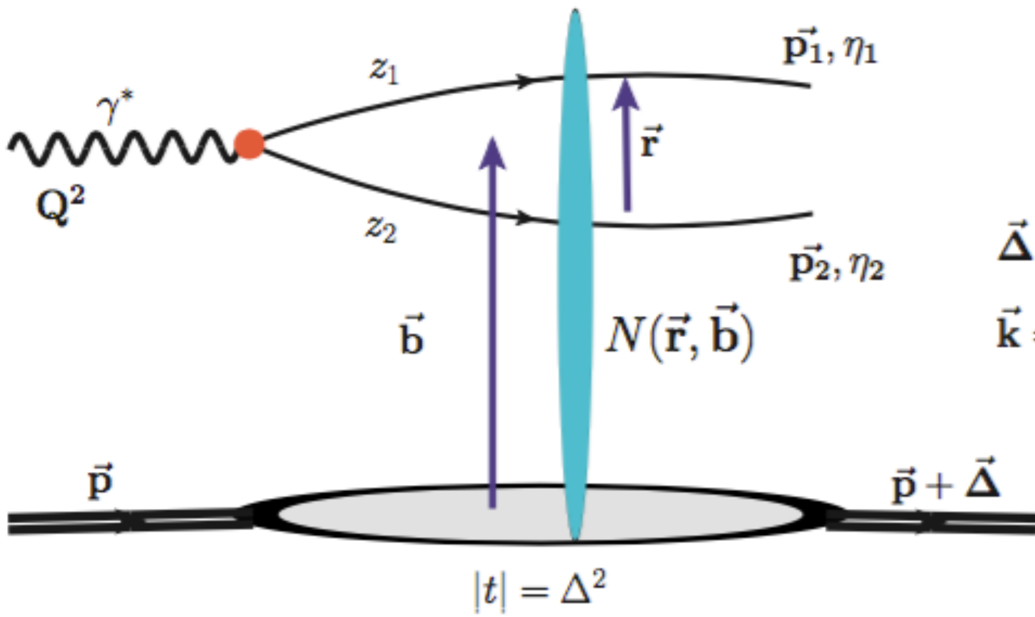

$\vec{\Delta} = \vec{p}_1 + \vec{p}_2$

$\vec{k} = \frac{1}{2}(\vec{p}_1 - \vec{p}_2)$

$$\sigma = \psi^{\gamma}_{q\bar{q}} \otimes \mathcal{N}(\vec{r}, \vec{b}) \otimes \mathcal{N}(\vec{r'}, \vec{b'}) \neq \psi^{\gamma}_{q\bar{q}} \otimes [\mathcal{N}(r, b)]^2$$

$$\left(\frac{d\sigma_{\mathrm{T}}^{\mathrm{dijet}}}{dz_1\, dz_2\, d^2\mathbf{p}_1 d^2\mathbf{p}_2}\right) = (2\pi)^2 \delta(z_1 + z_2 - 1) N_c \alpha_{em} \sum_f e_f^2 \int \frac{d^2\mathbf{r}}{(2\pi)^2} \int \frac{d^2\mathbf{r}'}{(2\pi)^2} \int \frac{d^2\mathbf{b}}{(2\pi)^2} \int \frac{d^2\mathbf{b}'}{(2\pi)^2}$$

$$\times\, \mathbf{e}^{-i(\mathbf{b}-\mathbf{b}')\cdot(\mathbf{p}_1+\mathbf{p}_2)} \mathbf{e}^{-i(\mathbf{r}-\mathbf{r}')\cdot(\mathbf{p}_1-\mathbf{p}_2)/2} \mathcal{N}(\mathbf{r}, \mathbf{b})\, \mathcal{N}(\mathbf{r}', \mathbf{b}')\, 2[z_1^2 + z_2^2]\, \frac{\mathbf{r}\cdot\mathbf{r}'}{\mathbf{r}^2 \mathbf{r}'^2}\, [\varepsilon|\mathbf{r}|K_1(\varepsilon|\mathbf{r}|)]\, \left[\varepsilon|\mathbf{r}'|K_1(\varepsilon|\mathbf{r}'|)\right]$$

- **Diffractive dijet production is a sensitive probe of the color-dipole orientation.**

Diffractive dijet production as a probe of color-dipole orientation

Inspired by "saturation domain" picture of Kovner & Lublinsky (2011)

$$\mathcal{N}(\mathbf{r},\mathbf{b}) = \mathcal{N}(r,b,\theta_r-\theta_b) = 1 - e^{-\frac{Q_s^2(b)}{4} r^2 \left(1+\mathbf{A}\cos^2(\theta_r-\theta_b)\right)}$$

θ_r, θ_b are the angles of vectors $\vec{r}$, $\vec{b}$ with respect to a reference vector, respectively. Assuming $Q_s^2 r^2 A/4 \ll 1$:

$$\int \frac{d^2\mathbf{r}}{(2\pi)^2} \int \frac{d^2\mathbf{b}}{(2\pi)^2} e^{-i\mathbf{b}\cdot(\mathbf{p}_0+\mathbf{p}_1)} e^{-i\mathbf{r}\cdot(\mathbf{p}_0-\mathbf{p}_1)/2} \mathcal{N}(\mathbf{r},\mathbf{b}) K_0(\varepsilon|\mathbf{r}|) \simeq \int_0^{+\infty} \frac{dr}{2\pi} r \int_0^{+\infty} \frac{db}{2\pi} b\, J_0\left(b|\mathbf{p}_0+\mathbf{p}_1|\right) \times J_0\left(r\frac{|\mathbf{p}_0-\mathbf{p}_1|}{2}\right) \mathcal{N}(r,b,\theta_- - \theta_+) K_0(\varepsilon r)$$

θ_+, θ_- denote the angles of vectors $\vec{\Delta} = \vec{p}_0 + \vec{p}_1$ and $\vec{k} = \frac{1}{2}(\vec{p}_0 - \vec{p}_1)$ with respect to a reference vector, respectively.

- **A nonzero A corresponding to the existence of $\vec{r} - \vec{b}$ correlations in the color dipole amplitude, induces azimuthal correlations between $\vec{\Delta}$ and $\vec{k}$.**

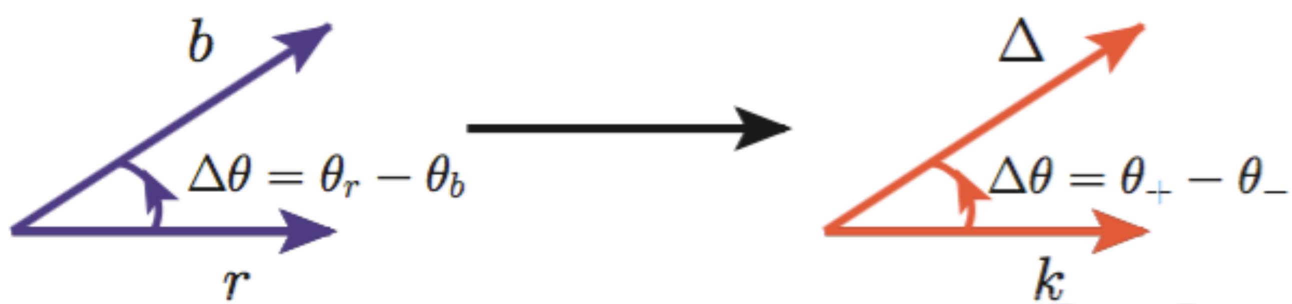

Diffractive dijet production as a probe of color-dipole orientation

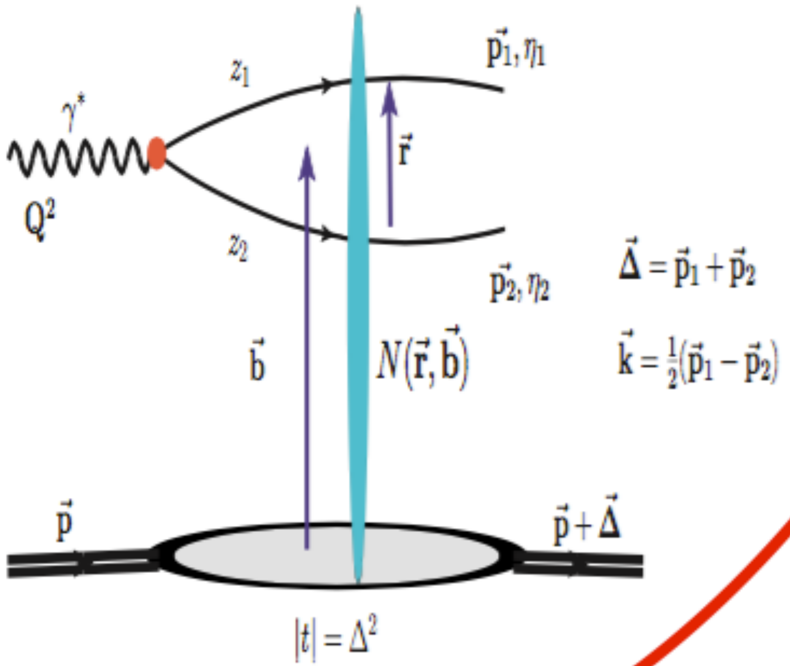

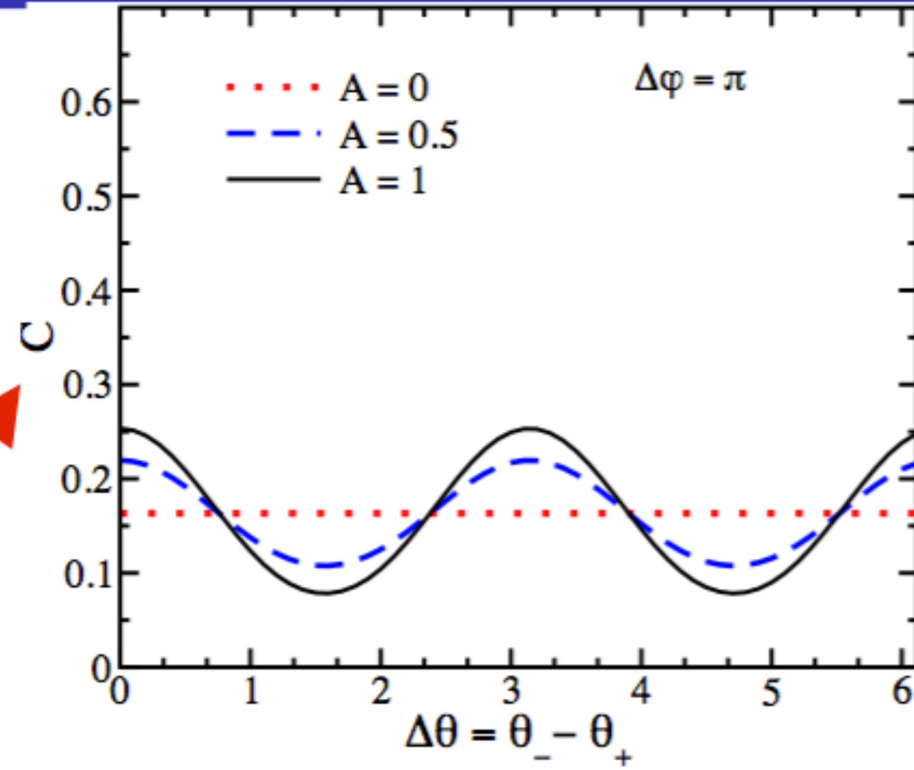

$$C(\Delta\theta) = \frac{d\sigma^{\gamma^* p \to q\bar{q}p}}{d\mathbf{p}_0\, \mathbf{p}_1 d\Delta\theta} \Big/ \int_0^{2\pi} d\Delta\theta \frac{d\sigma^{\gamma^* p \to q\bar{q}p}}{d\mathbf{p}_0\, \mathbf{p}_1 d\Delta\theta}$$

- **A nonzero A corresponding to the existence of $\vec{r} - \vec{b}$ correlations in the color dipole amplitude, induces sizeable azimuthal correlations for dijet between $\vec{\Delta}$ and $\vec{k}$.**

Color-dipole orientation as an origin of elliptic flow in pp and pA collisions

Iancu-Rezaeian (to show up on Archive Feb 15, 2017)

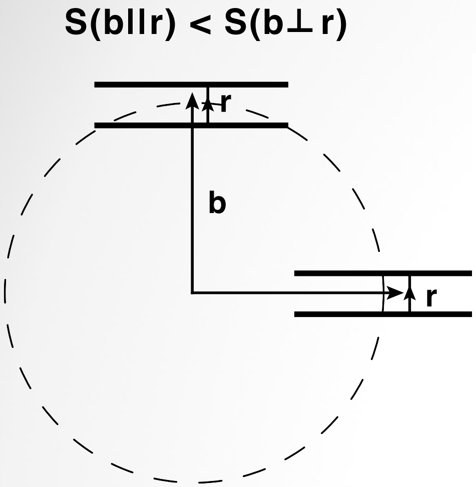

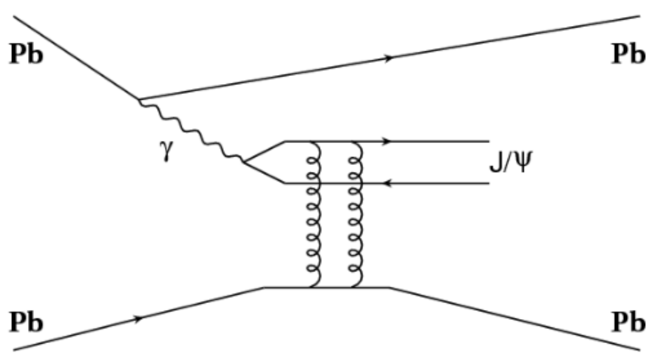

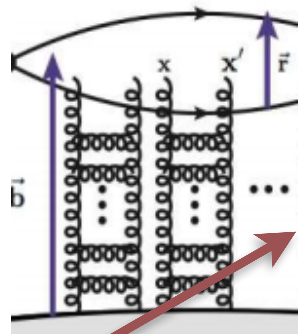

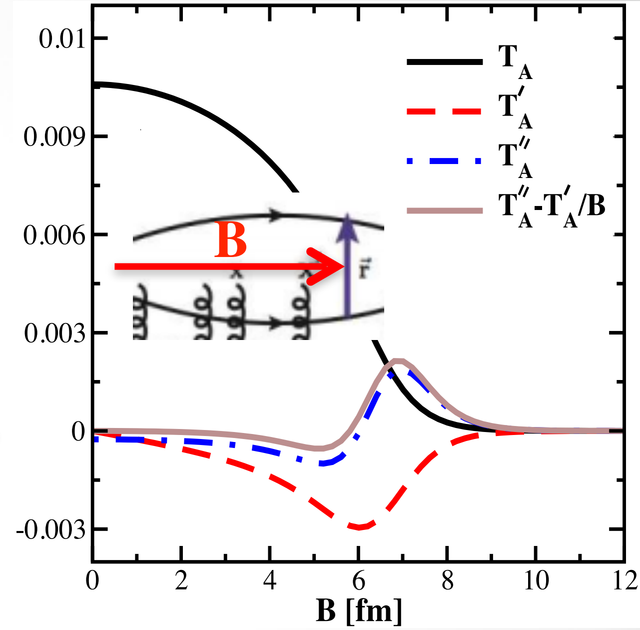

The color-dipole orientation probes the inhomogeneity of the target in the transverse plane.

$$N_{2g}^A(B,r,\theta) = \mathcal{N}_0^A(B,r) + \mathcal{N}_\theta^A(B,r)\cos(2\theta),$$

Original McLerran-Venugopalan model

$$\mathcal{N}_0^A(B,r) = \pi R^2 Q_{0s}^2 r^2 \ln\left(\frac{1}{r^2m^2}+\mathrm{e}\right)\left[T_A(B) + R^2\left(T_A''(B)+\frac{1}{B}T_A'(B)\right)\right] + \frac{\pi}{3}\frac{R^2}{m^2}Q_{0s}^2 r^2\left(T_A''(B)+\frac{1}{B}T_A'(B)\right),$$

$$\mathcal{N}_\theta^A(B,r) = \frac{\pi}{6}\frac{R^2}{m^2}Q_{0s}^2 r^2\left(T_A''(B)-\frac{1}{B}T_A'(B)\right).$$

$$v_2(p,B) = \frac{\int r\mathrm{d}r\, \mathrm{e}^{-A\mathcal{N}_0^A(B,r)}\, \mathrm{J}_2(pr)\, \mathrm{I}_1\left(A\mathcal{N}_\theta^A(B,r)\right)}{\int r\mathrm{d}r\, \mathrm{e}^{-A\mathcal{N}_0^A(B,r)}\, \mathrm{J}_0(pr)\, \mathrm{I}_0\left(A\mathcal{N}_\theta^A(B,r)\right)}.$$

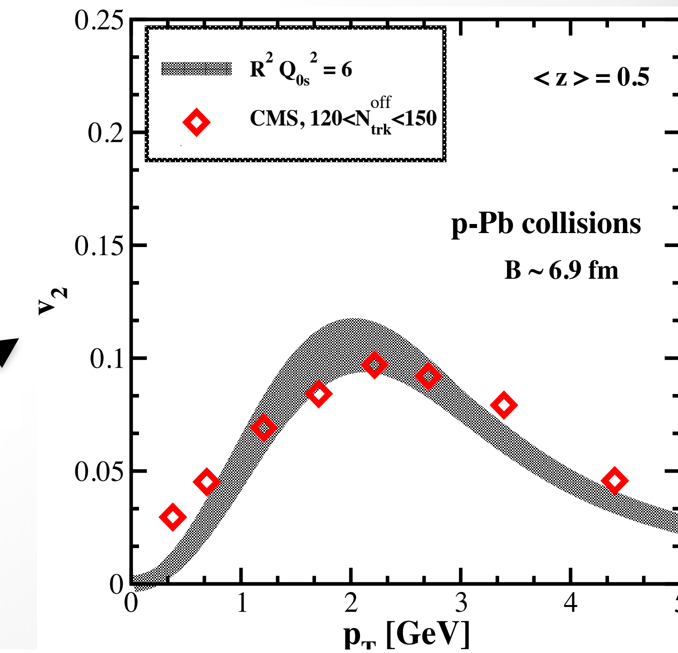

Color-dipole orientation as an origin of elliptic flow in pp and pA collisions

Iancu-Rezaeian (to show up on Archive Feb 15, 2017)

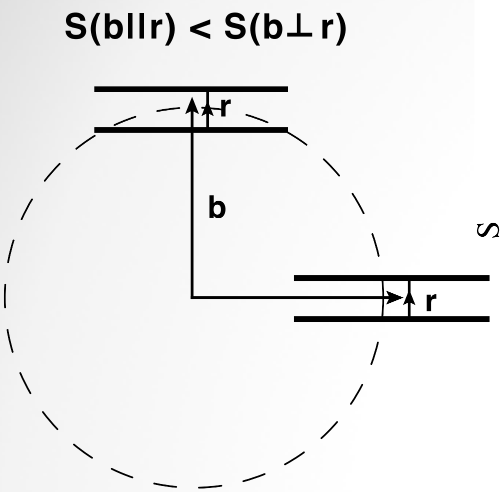

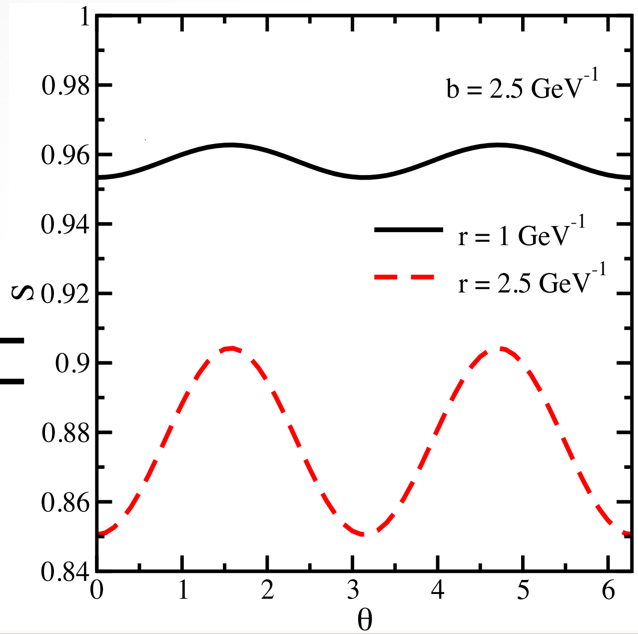

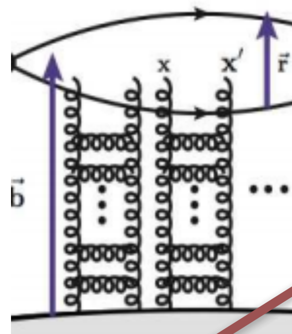

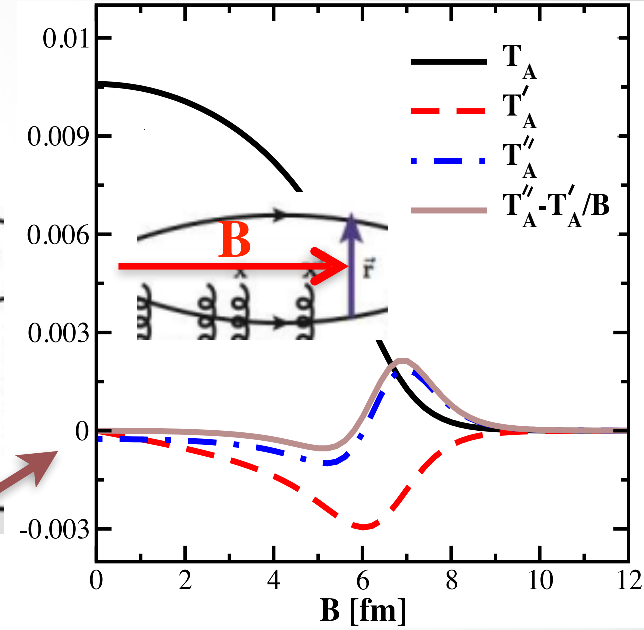

The color-dipole orientation probes the inhomogeneity of the target in the transverse plane.

$$N_{2g}^{A}(B,r,\theta) = \mathcal{N}_0^A(B,r) + \mathcal{N}_\theta^A(B,r)\cos(2\theta),$$

Original McLerran-Venugopalan model

$$\mathcal{N}_0^A(B,r) = \pi R^2 Q_{0s}^2 r^2 \ln\left(\frac{1}{r^2 m^2} + \mathrm{e}\right)\left[T_A(B) + R^2\left(T_A''(B) + \frac{1}{B}T_A'(B)\right)\right] + \frac{\pi}{3}\frac{R^2}{m^2}Q_{0s}^2 r^2\left(T_A''(B) + \frac{1}{B}T_A'(B)\right),$$

$$\mathcal{N}_\theta^A(B,r) = \frac{\pi}{6}\frac{R^2}{m^2}Q_{0s}^2 r^2\left(T_A''(B) - \frac{1}{B}T_A'(B)\right).$$

$$v_2(p,B) = \frac{\int r\mathrm{d}r\, \mathrm{e}^{-A\mathcal{N}_0^A(B,r)}\, \mathrm{J}_2(pr)\, \mathrm{I}_1\left(A\mathcal{N}_\theta^A(B,r)\right)}{\int r\mathrm{d}r\, \mathrm{e}^{-A\mathcal{N}_0^A(B,r)}\, \mathrm{J}_0(pr)\, \mathrm{I}_0\left(A\mathcal{N}_\theta^A(B,r)\right)}.$$

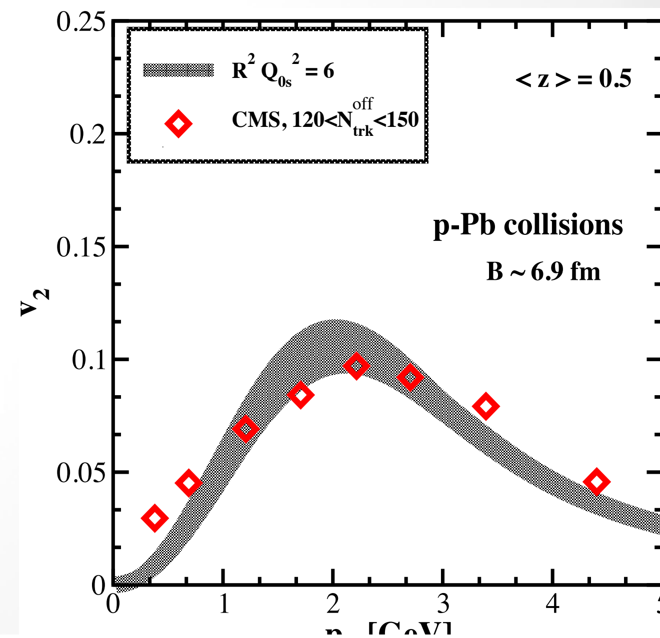

Color-dipole orientation as an origin of elliptic flow in pp and pA collisions

Iancu-Rezaeian (to show up on Archive Feb 15, 2017)

The anisotropy due to the color-dipole orientation mechanism is universal for different processes in dilute-dense scatterings.

There will be the analog of azimuthal anisotropy v_n in DIS and UPC.

Stay tuned!.

The color-dipole orientation probes the inhomogeneity of the target in the transverse plane.

$$N_{2g}^A(B,r,\theta) = \mathcal{N}_0^A(B,r) + \mathcal{N}_\theta^A(B,r)\cos(2\theta),$$

Original McLerran-Venugopalan model

$$\mathcal{N}_0^A(B,r) = \boxed{\pi R^2 Q_{0s}^2 r^2 \ln\left(\frac{1}{r^2m^2}+\mathrm{e}\right)}\left[T_A(B) + R^2\left(T_A''(B)+\frac{1}{B}T_A'(B)\right)\right] + \frac{\pi}{3}\frac{R^2}{m^2}Q_{0s}^2r^2\left(T_A''(B)+\frac{1}{B}T_A'(B)\right),$$

$$\mathcal{N}_\theta^A(B,r) = \frac{\pi}{6}\frac{R^2}{m^2}Q_{0s}^2r^2\left(T_A''(B)-\frac{1}{B}T_A'(B)\right).$$

$$v_2(p,B) = \frac{\int r\mathrm{d}r\, \mathrm{e}^{-A\mathcal{N}_0^A(B,r)}\, \mathrm{J}_2(pr)\, \mathrm{I}_1\left(A\mathcal{N}_\theta^A(B,r)\right)}{\int r\mathrm{d}r\, \mathrm{e}^{-A\mathcal{N}_0^A(B,r)}\, \mathrm{J}_0(pr)\, \mathrm{I}_0\left(A\mathcal{N}_\theta^A(B,r)\right)}.$$

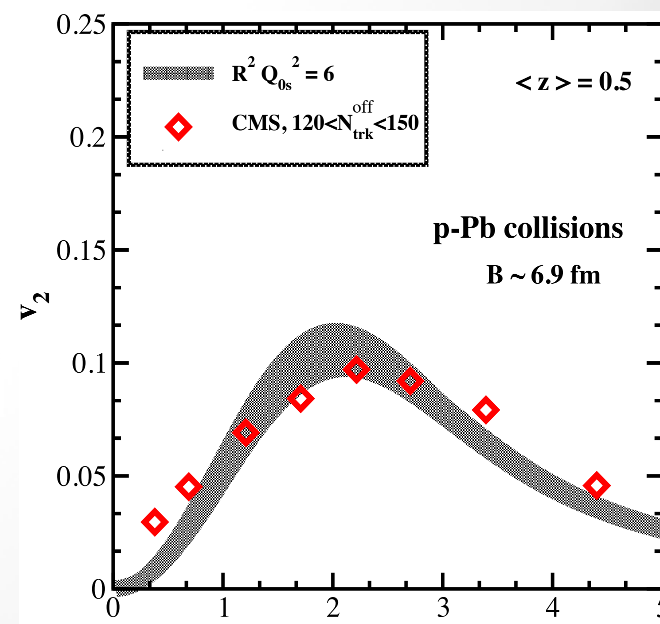

Correlations v. decorrelations

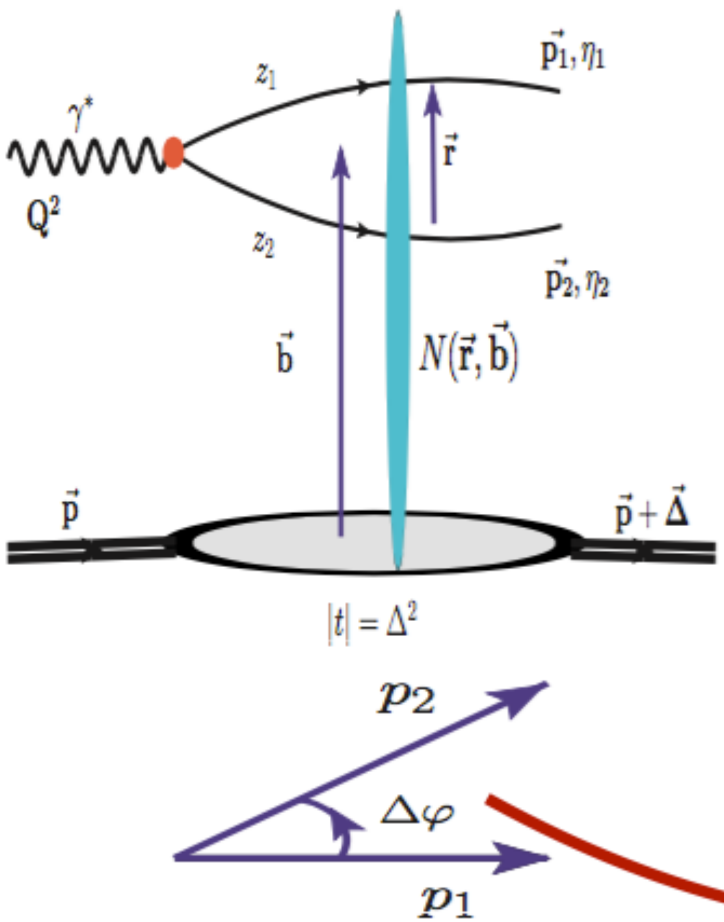

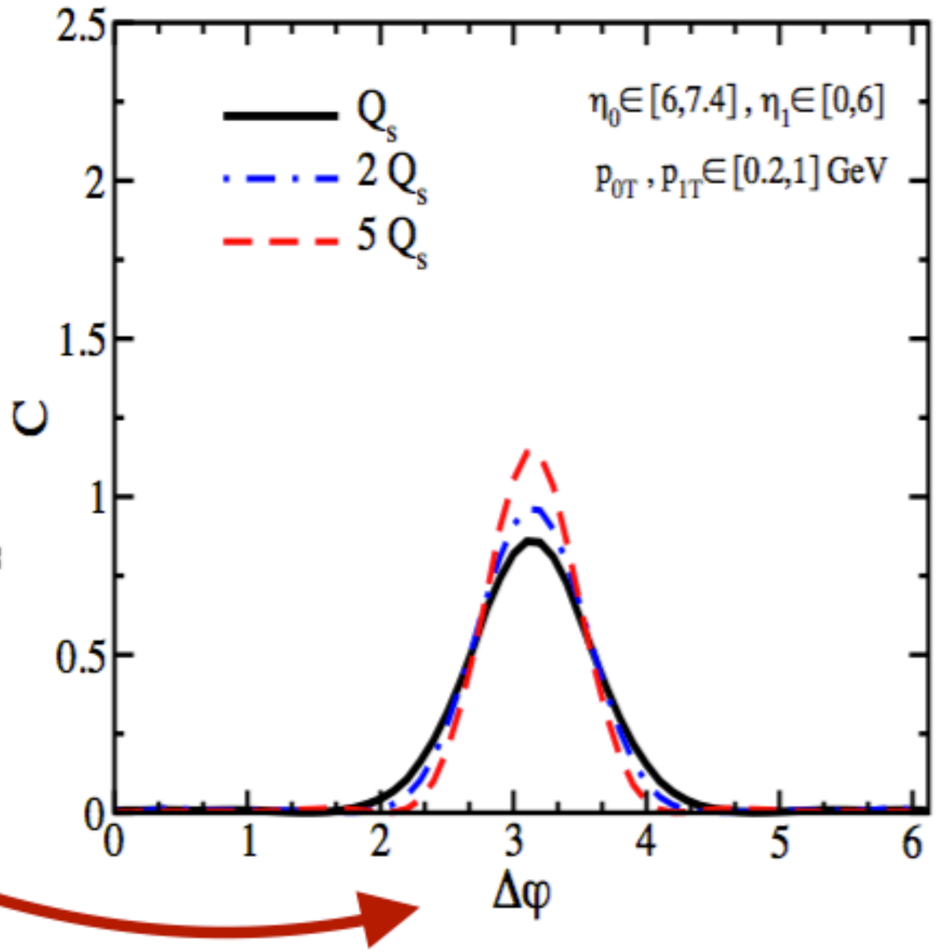

- In order to keep the color neutrality of the dijet system, required by its diffractive nature, the production becomes dominated by $q\bar{q}$ pairs of smaller transverse size with increasing saturation momentum.

Inclusive v. diffractive two-particle production

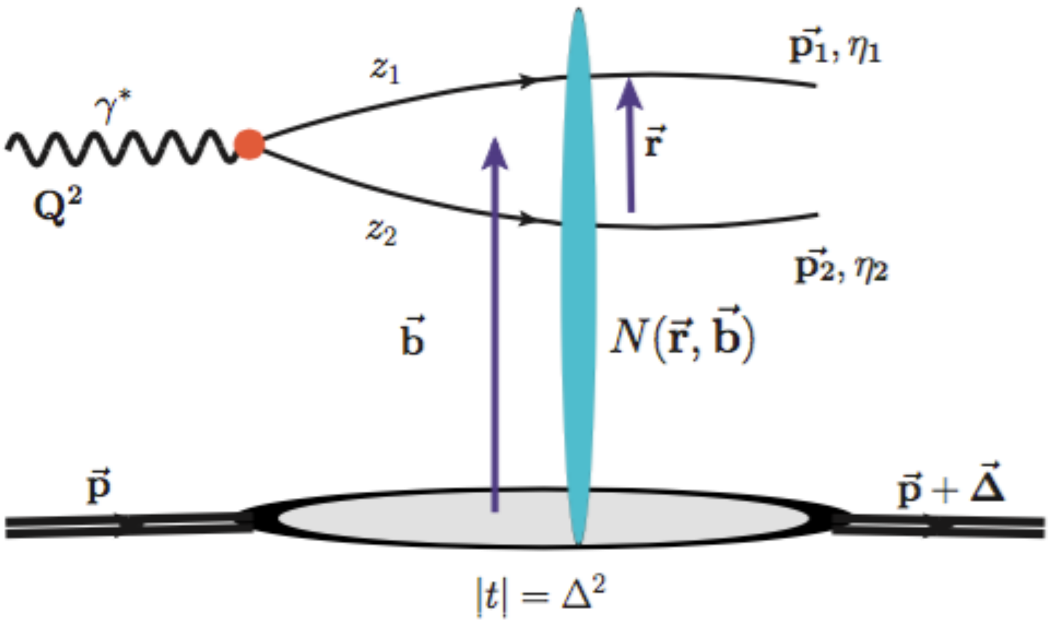

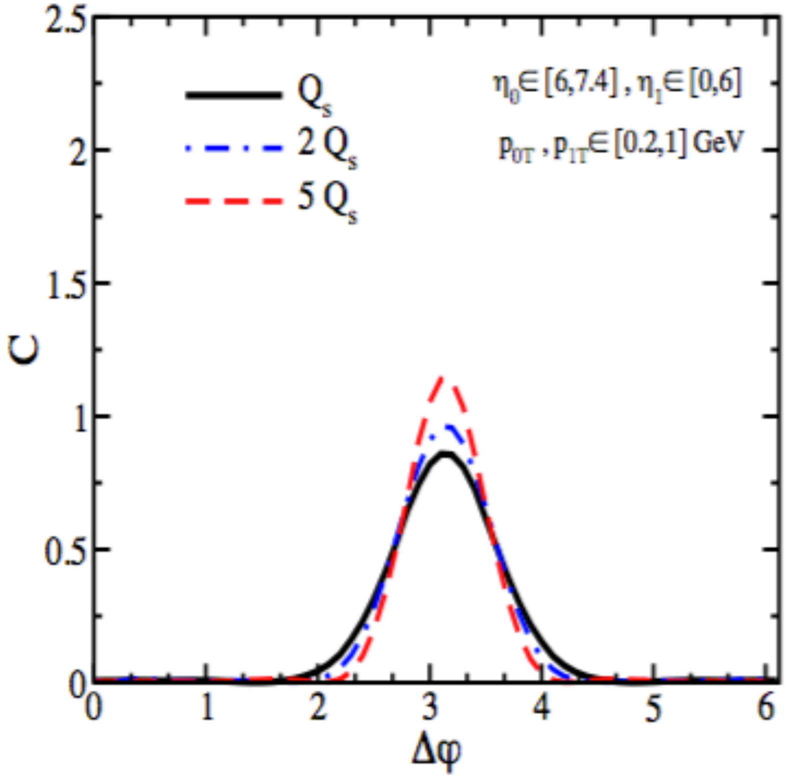

- **Diffractive** dijet photoproduction:
  Back-to-back correlation gets **enhanced** due to the saturation scale.
  Balance between: $p_{1T}, p_{2T}, \vec{\Delta}, Q_s$
- **Inclusive** dijet:
  Back-to-back correlation gets **suppressed** due to the saturation scale.
  Balance between: p_{1T}, p_{2T}, Q_s

$$\vec{\Delta} = \vec{p_1} + \vec{p_2}, \quad \vec{k} = \frac{1}{2}(\vec{p_1} - \vec{p_2}), \quad |t| = \Delta^2, \; |t| \propto 1/b$$

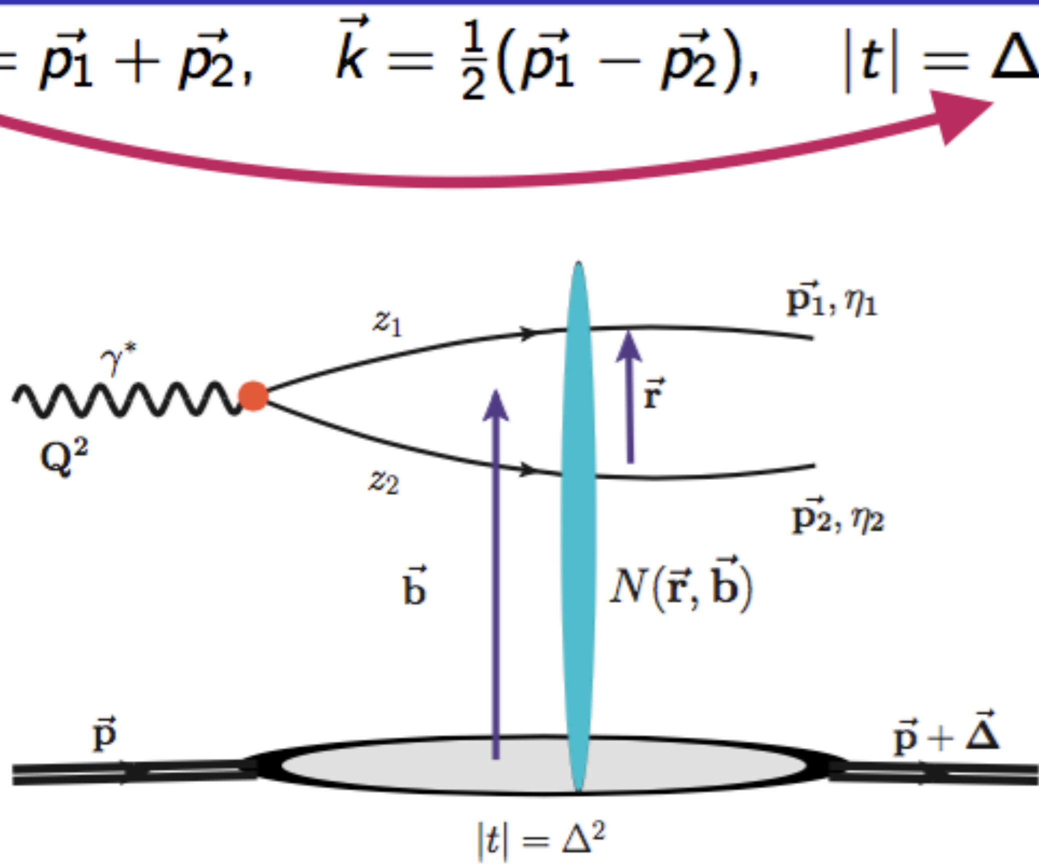

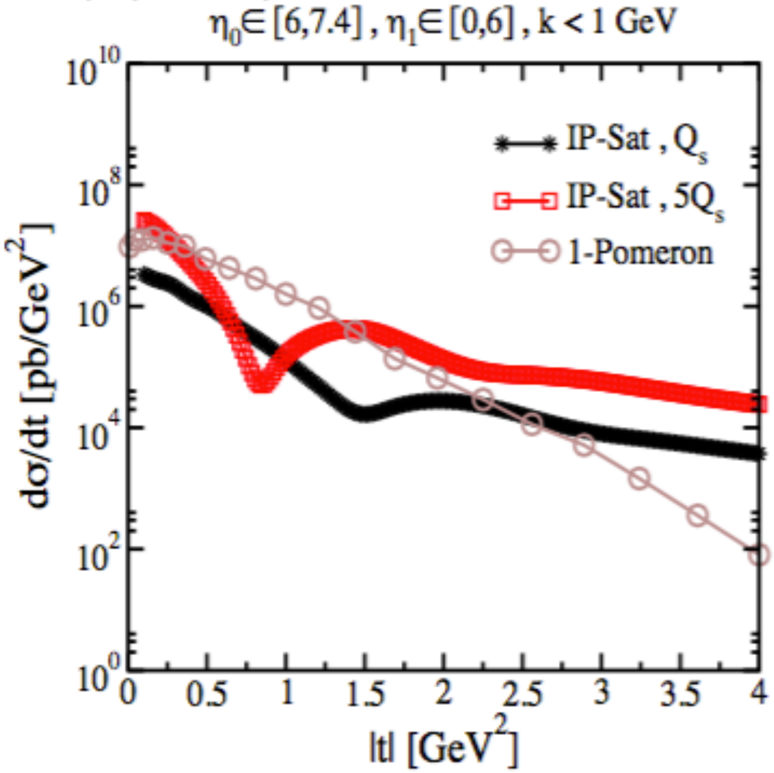

Diffractive dijet photoproduction:

- $|t|$ distribution exhibits dips for the saturation models, similar to diffractive vector mesons.
- There is NO dips for the non-saturation models (i.e. 1-Pomeron).
- The dips become stronger by increasing the saturation scale.

The origin of diffractive dips: Non-linear evolution of black-disc region

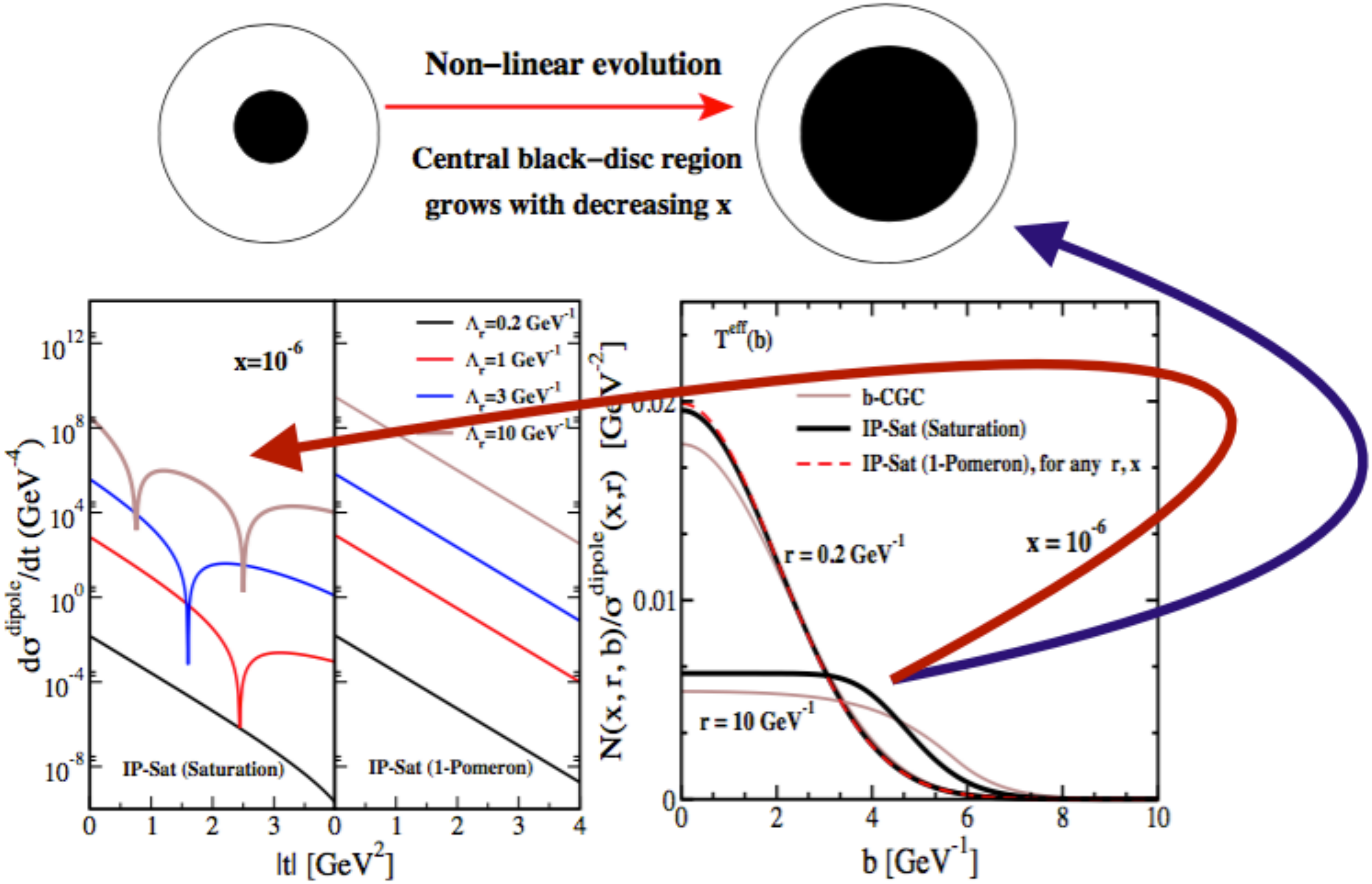

- Non-linear evolution $\Longrightarrow$ evolves any realistic profile in b, like a Gaussian or Woods-Saxon distribution, and makes it closer to a step-like function in the b-space at black-disc limit.

The universality of the diffractive dip at small-x

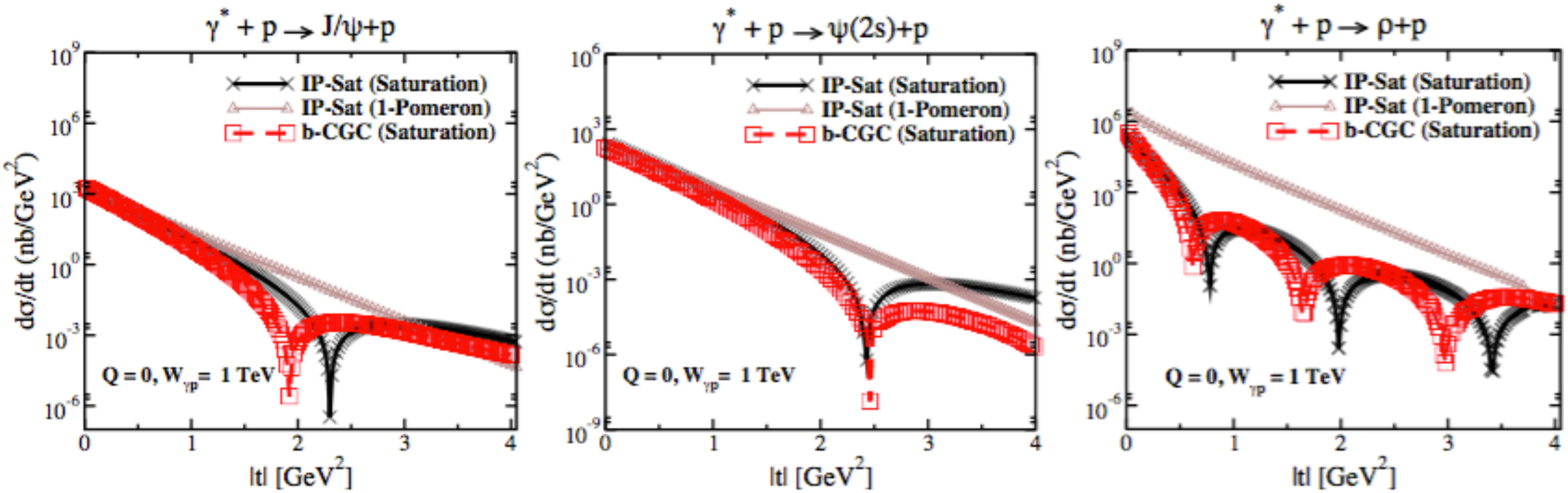

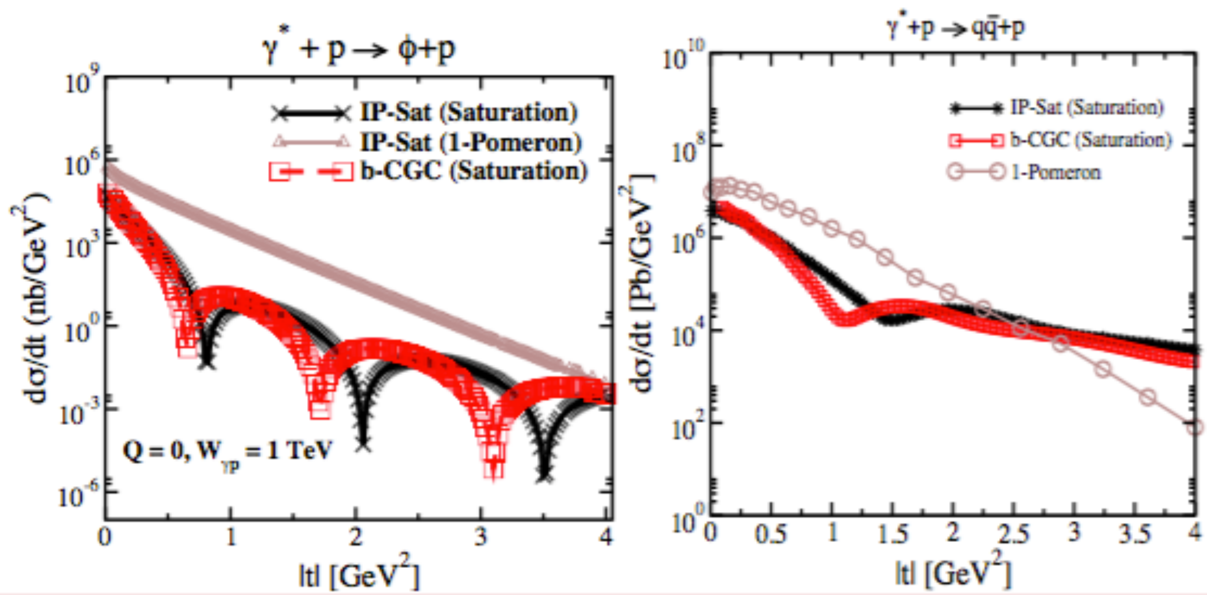

Armesto, AR
arXiv:1402.4831

- The emergence of dip structure in the diffractive t-distribution is universal and does not depend on the details of the final-state particle wave functions.

Main conclusion: Small-x gluon tomography in diffractive dijet in UPC

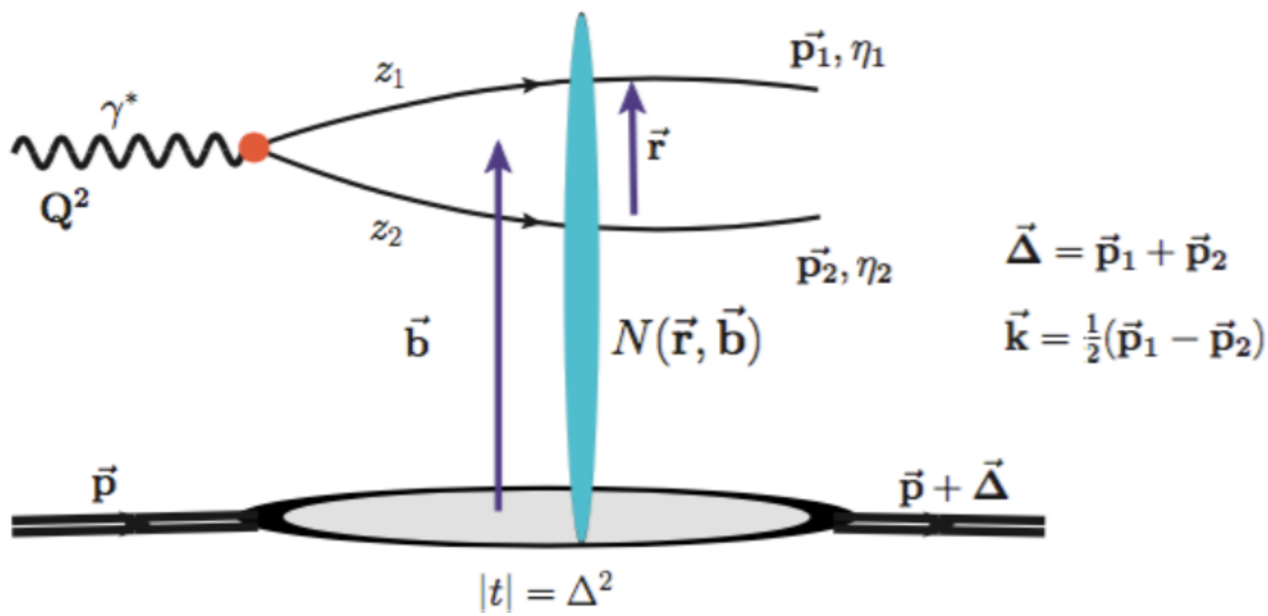

✦ **Correlations between $\vec{p}_1$, $\vec{p}_2$ probe the effective dipole size $r \approx 1/Q_s(b)$.**

✦ **Correlation between $\vec{k}, \vec{\Delta}$ probe the color-dipole orientation and correlations between $\vec{r}, \vec{b}$.**

✦ **t-distribution of the diffractive dijet photo-production probes the inhomogeneity of the target.**

Altinoluk, Armesto, Beuf, and Rezaeian, PLB 758 (2016) 373.
Hatta, Xiao and Yuan, PRL 116 (2016) 202301.